Modeling heat transfer in gas-particle mixtures: Calculation of the macro-scale heat exchange in Eulerian–Lagrangian approaches using spatial averaging

Mohamed Belerrajoul, Yohan Davit, Michel Quintard, Olivier Simonin, Fabien Duval

Modeling heat transfer in gas-particle mixtures: Calculation of the macro-scale heat exchange in Eulerian–Lagrangian approaches using spatial averaging

Mohamed Belerrajoul[a,b], Yohan Davit[a], Michel Quintard[a], Olivier Simonin[a], Fabien Duval[b,*]

[a] CNRS, Institut de Mécanique des Fluides de Toulouse (IMFT), Université de Toulouse, Toulouse, France
[b] Institut de Radioprotection et de Sûreté Nucléaire (IRSN), Saint Paul Lez Durance 13115, France

Keywords:
Euler-Lagrange methods
Upscaling
Volume averaging
Heat transfer
Closure problems

A B S T R A C T

Heat transfers in dilute gas-particle mixtures are often modeled using hybrid Euler–Lagrange descriptions, treating the carrier fluid via an Eulerian representation and following each particle in a Lagrangian framework. One of the focal issues in these models is the calculation of the macro-scale heat transfer between the continuous phase and particles. In the standard approach, the heat transfer for each particle is considered to vary linearly with the average temperature difference between the particle and the fluid. Here, we use the method of volume averaging with closure to filter the heat transfer equations at the micro-scale and derive a closed form of the heat transfer rate, which is significantly different from the standard case. The primary difference is that the heat transfer for a given particle does not only depend on the temperature of the particle but also depends on the temperatures of all other particles within the averaging volume. This yields a matrix of heat exchange coefficients that captures indirect particle–particle exchanges at macro-scale. Using simple model cases, we validate our approach, compare it to the standard heat transfer model and show that it degenerates toward the standard model only in specific cases.

1. Introduction

We are interested in dust explosion hazard in the context of nuclear safety and, in particular, in modeling flame propagation for dilute and dispersed gas-particle flows with particle sizes typically ranging from 10^{-6} to 10^{-4} m and a volume fraction of particles up to 10^{-3}. Such configurations correspond to accident scenarios that may happen during operations of decommissioning of uranium natural graphite gas reactors (D'Amico et al., 2016) that involve graphite particles or loss of vacuum accident in the vessel of fusion reactors (Denkevits and Dorofeev, 2005; Janeschitz, 2001) that involve either tungsten or beryllium particles. In this context, an important modeling issue is to identify the mechanisms that influence the severity of the explosion and may result in the release of radioactive or toxic materials.

Our global strategy follows the ones proposed in e.g., Cannevière (2003) and Neophytou and Mastorakos (2009) for liquid fuel droplets or in Cloney et al. (2018) and Park and Park (2016) for coal particles. The idea is to use detailed numerical simulations to analyze the flame structure and calculate the laminar burning velocity that is then used in a second step to determine the turbulent flame velocity (see for instance Proust, 2017; Silvestrini et al., 2008). Detailed numerical simulations are often computed via a hybrid Euler–Lagrange description, which uses a filtered Eulerian representation of the fluid phase and a Lagrangian tracking of the particles (Boivin et al., 2000; Capecelatro and Desjardins, 2013; Crowe et al., 2011; Simonin et al., 1993). In this context, the macro-scale energy balance equations are written classically as

$$\partial_t\left(\alpha_\beta(\rho c_p)_\beta\langle T_\beta\rangle^\beta\right)+\nabla\cdot\left(\alpha_\beta(\rho c_p)_\beta\langle T_\beta\rangle^\beta\langle\mathbf{u}_\beta\rangle^\beta\right)$$
$$=\nabla\cdot\left(\alpha_\beta\lambda^*_\beta\nabla\langle T_\beta\rangle^\beta\right)-\frac{1}{\mathcal{V}}\sum_{p=1}^{N_\mathcal{V}}Q_{\beta p} \tag{1}$$

$$(mc_p)_p\frac{dT_p}{dt}=Q_{\beta p} \tag{2}$$

The first equation corresponds to the heat transfer equation for the filtered temperature $\langle T_\beta\rangle^\beta$ of the continuous β-phase, where λ^*_β, $\langle\mathbf{u}_\beta\rangle^\beta$, $(\rho c_p)_\beta$ and α_β are respectively an effective thermal conductivity, the intrinsic velocity, the volumetric heat

* Corresponding author.
E-mail address: fabien.duval@irsn.fr (F. Duval).

Nomenclature

Roman letters

A_p	surface area of a particle, m^2
$A_{\beta\sigma}$	interfacial area of the $\beta-\sigma$ contained within the averaging volume, m^2
a_v	interfacial area per unit volume, m^{-1}
$\mathrm{Bi}_p = h_p d_p/\lambda_\sigma$	particle Biot number
$\mathbf{b}_\beta$	vector that maps $\nabla\langle T_\beta\rangle^\beta$ onto $\widetilde{T}_\beta$, m
c_p	specific heat capacity, $J\,kg^{-1}\,K^{-1}$
d_p	particle diameter, m
h_{pj}	heat exchange coefficients, $W\,m^{-2}\,K^{-1}$
$\mathbf{K}_\beta$	effective thermal dispersion tensor, $W\,m^{-1}\,K^{-1}$
l_β	characteristic length (micro-scale) for the β-phase, m
L_β	macroscopic characteristic length, m
m_p	particle mass, kg
g	weighting function
$N_\mathcal{V}$	number of particles contained in the averaging volume $\mathcal{V}$
$\mathbf{n}_{\beta\sigma}$	unit normal vector from the β-phase towards the σ-phase
$Q_{\beta p}$	macro-scale heat transfer rate between the continuous phase and particle p, W
$\mathbf{r}$	position vector, m
r_g	radius of the averaging volume, m
s_p	scalar that maps $\langle T_\beta\rangle^\beta - T_j$ onto $\widetilde{T}_\beta$
T_η	$\eta=\beta,\sigma$, temperature in the η-phase, K
T_p	particle temperature, K
$\langle T_\beta\rangle^\beta$	intrinsic average temperature for the β-phase, K
$\widetilde{T}_\beta$	deviation temperature for the β-phase, K
T_β^0	undisturbed temperature for the β-phase, K
t^*	characteristic time associated with the micro-scale diffusion, s
$\mathbf{u}_\beta$	velocity in the β-phase, $m\,s^{-1}$
$\langle\mathbf{u}_\beta\rangle^\beta$	intrinsic average velocity for the β-phase, $m\,s^{-1}$
$\widetilde{\mathbf{u}}_\beta$	deviation velocity for the β-phase, $m\,s^{-1}$
$\mathcal{V}$	averaging volume, m^3
$\mathbf{x}_p$	particle position, m

Greek letters

λ_β	thermal conductivity for the β-phase, $W\,m^{-1}\,K^{-1}$
ω_σ	volumetric heat source, $W\,m^{-3}$
ρ_η	$\eta=\beta,\sigma$, density for the η-phase, $kg\,m^{-3}$
α_η	$\eta=\beta,\sigma$, volume fraction of the η-phase
$\delta_{\beta\sigma}$	Dirac distribution associated with the $\beta-\sigma$ interface
γ_β	indicator function for the β-phase
β	continuous phase
σ	dispersed phase
ξ	Laplace variable, s^{-1}

Superscripts

∞	quasi-steady
$*$	time convolution product

capacity and the volume fraction of the β-phase. The last term in Eq. (1) corresponds to the macro-scale heat transfer rate between the continuous phase and the $N_\mathcal{V}$ particles contained within the averaging volume $\mathcal{V}$. For the pth-particle, the corresponding heat transfer reads

$$Q_{\beta p} = \int_{A_p} \mathbf{n}\cdot\lambda_\beta\nabla T_\beta\,\mathrm{d}S \tag{3}$$

where A_p is the surface of particle p and $\mathbf{n}$ denotes the outward unit normal vector on the particle surface A_p.

The second equation in the Euler–Lagrange description Eq. (2) describes the averaged particle temperature T_p, where $(mc_p)_p$ is the product of the mass and heat capacity of the pth-particle. The model for the macro-scale heat transfer $Q_{\beta p}$ is usually based on the description of heat transfer in the case of an isolated particle (Michaelides and Feng, 1994). To solve the heat transfer problem, this description uses a decomposition of the surrounding phase temperature into an undisturbed temperature and a disturbance due to the presence of the particle. Generalizing from an isolated particle to a set of particles, the undisturbed temperature is often viewed as a macro-scale temperature $\langle T_\beta\rangle^\beta$ and the resulting heat exchange reads (Ling et al., 2016; Michaelides and Feng, 1994)

$$Q_{\beta p} = \int_{A_p} \mathbf{n}\cdot\lambda_\beta\nabla\langle T_\beta\rangle^\beta\,\mathrm{d}S + A_p h_p\left(\langle T_\beta\rangle^\beta - T_p\right) + A_p\int_0^t K_p(\tau)\,\frac{d\left(\langle T_\beta\rangle^\beta - T_p\right)}{d\tau}\,\mathrm{d}\tau \tag{4}$$

In Eq. (4), the first term refers to the undisturbed heat flux seen by the particle. It represents the flux that would have entered the volume occupied by the continuous phase in the absence of the particle. The second term corresponds to the quasi-steady heat transfer from the particle to the surrounding phase due to temperature difference. The heat exchange coefficient h_p between the continuous phase and the particle is usually expressed in terms of the particle Nusselt number as $\mathrm{Nu}_p = h_p d_p/\lambda_\beta$ for which numerous empirical functions of the particle Reynolds number have been proposed (see for instance Ranz and Marshall, 1952; Whitaker, 1972) with the asymptotic limit $\mathrm{Nu}_p = 2$ when the particle Reynolds number effect can be neglected. The last term in Eq. (4) is non-local and captures history effects due to the transient development of the temperature in the particle vicinity. The kernel function $K_p(\tau)$ that appears in the history integral has been calculated analytically in Michaelides and Feng (1994) for an isolated particle without a velocity difference between the continuous phase and the particle, and the results have been extended to finite particle Reynolds number in Balachandar and Ha (2001) and Feng and Michaelides (1996). Usual simplifications of this problem include neglecting the non-local contribution to decrease the computational cost and replacing the first term by the time derivative of the undisturbed temperature (Ling et al., 2016; Michaelides and Feng, 1994).

In this work, our goal is to propose alternative expressions of the heat transfer rate using an up-scaling methodology based on spatial averaging with closure (Carbonell and Whitaker, 1984; Davit et al., 2013; Quintard and Whitaker, 2000). This methodology allows us to derive macro-scale equations that, unlike standard Euler–Lagrange approaches, take into account heat transfer between particles in the heat exchange $Q_{\beta p}$ through a matrix of heat exchange coefficients. To be more clear about heat transfer between particles, these have not to be confused with direct particle–particle exchanges that take place during collisions and that are negligible in the dilute regime considered in this work. Here, heat transfer between particles take place through the continuous carrier phase and thus will be referred as indirect particle–particle exchanges. The resulting heat exchange coefficients involve both a quasi-steady and a non-local contribution that captures history effects. Our approach further provides closure problems that link the effective transport coefficients to the micro-scale geometry. To recover more standard formulations, the problem can be simplified

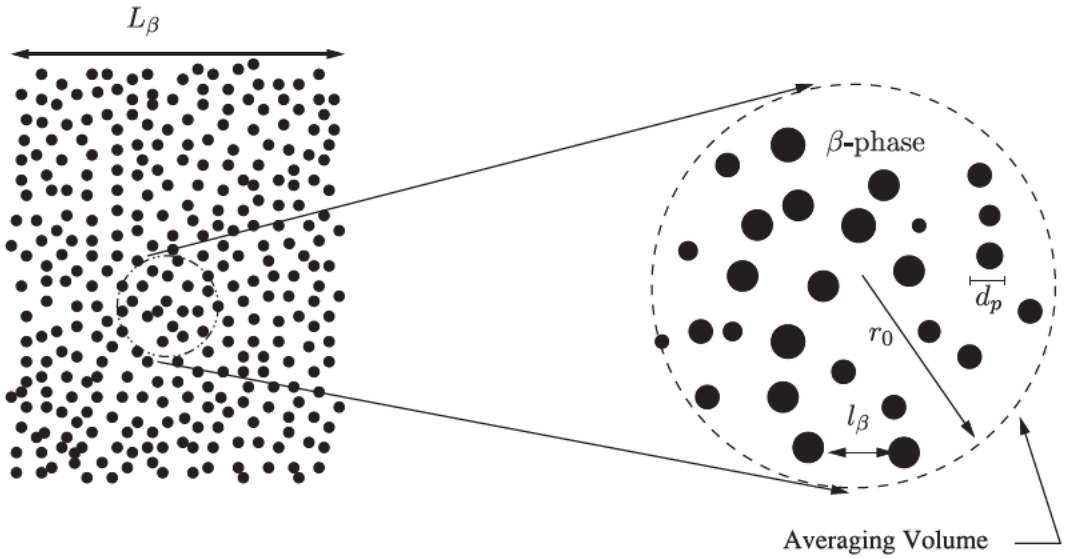

Fig. 1. Macroscopic region of a two-phase system and the corresponding averaging volume.

through quasi-steady approximations and a diagonalization of the heat exchange matrix. In the last part of this work, we validate our models and compare the different approaches for model one-, two- and three-dimensional configurations with immobile particles in a purely conductive setup. The macro-scale models are then compared together and to the results from the direct computations at the micro-scale.

2. Micro-scale heat transfer problem

We consider the problem of heat transfer in a dispersed two-phase system as represented in Fig. 1, together with a homogeneous heat source in the solid phase that mimics heat release from burning particles. The continuous phase is identified as the β-phase while the dispersed one is identified as the σ-phase. The dispersed phase consists of rigid spherical particles of diameter d_p. The physical properties of each phase are considered to be uniform and constant.

The micro-scale boundary value problem describing heat transfer reads

$$\partial_t\big((\rho c_p)_\beta T_\beta\big) + \nabla\cdot\big((\rho c_p)_\beta T_\beta \mathbf{u}_\beta\big) = \nabla\cdot\big(\lambda_\beta \nabla T_\beta\big), \quad \text{in the } \beta\text{-phase} \tag{5}$$

$$\mathbf{n}_{\beta\sigma}\cdot(\lambda_\beta\nabla T_\beta) = \mathbf{n}_{\beta\sigma}\cdot(\lambda_\sigma\nabla T_\sigma), \text{ at } A_{\beta\sigma} \tag{6}$$

$$T_\beta = T_\sigma, \text{ at } A_{\beta\sigma} \tag{7}$$

$$\partial_t((\rho c_p)_\sigma T_\sigma) + \nabla\cdot((\rho c_p)_\sigma T_\sigma \mathbf{u}_\sigma) = \nabla\cdot(\lambda_\sigma\nabla T_\sigma) + \omega_\sigma, \quad \text{in the } \sigma\text{-phase} \tag{8}$$

where λ_η, $(\rho c_p)_\eta$ and $\mathbf{u}_\eta$ are respectively the thermal conductivity, the volumetric heat and the velocity of the η-phase ($\eta = \beta, \sigma$). ω_σ denotes the homogeneous heat source that may depend on position but not on temperature. In the boundary conditions, Eqs. (6) and (7), $A_{\beta\sigma}$ refers to the $\beta-\sigma$ interface and $\mathbf{n}_{\beta\sigma}$ is the unit normal vector oriented from the β-phase towards the σ-phase.

We are primarily interested in dust mixtures for which the thermal conductivity of the σ-phase is much larger than that of the β-phase, typically $\lambda_\sigma/\lambda_\beta \sim 10^3$ for a mixture of graphite particles and air. In the remainder of this paper, we therefore assume that $\lambda_\sigma/\lambda_\beta \gg 1$. This implies that the particle Biot number is much smaller than unity ($\mathrm{Bi}_p \ll 1$), so that the temperature of the σ-phase is considered uniform within each particle.

3. Macro-scale Eulerian–Lagrangian equations

3.1. Average equations

In a macro-scale Eulerian–Lagrangian description, the fluid is described as a continuous phase while the solid phase is treated by a Lagrangian tracking of each particle. The dispersed and continuous phases exchange heat through transfer terms in the transport equations. Since the characteristic size d_p of each particle is much smaller than a characteristic macroscopic lengthscale L_β, such exchange terms cannot be directly determined from a detailed computation of temperature gradients in the vicinity of each particle and require the development of specific models. To derive these models, we use an up-scaling methodology that consists in applying a spatial filter to the micro-scale heat transfer problem for the continuous phase at a scale r_g, such that $d_p \ll r_g \ll L_\beta$ (see for instance Anderson and Jackson, 1967; Capecelatro and Desjardins, 2013; Carbonell and Whitaker, 1984). Here, we use the method of volume averaging with closure and only the main steps of the methodology are outlined below, since this approach has been extensively discussed in the literature (Davit and Quintard, 2015; Quintard and Whitaker, 1993a; 2000; Whitaker, 1998).

First, a spatial averaging operator is defined at point $\mathbf{x}$ for a function ψ_β associated with the β-phase as

$$\langle\psi_\beta\rangle = g * \psi_\beta = \int_{\mathbb{R}^d} g(\mathbf{x}-\mathbf{r})\psi_\beta(\mathbf{r})\,\mathrm{d}\mathbf{r} \tag{9}$$

where g is a kernel defining the properties of the spatial filtering. To localize the average, we generally require that g has compact support in $\mathbb{R}^d$ with a characteristic lengthscale r_g. For simplicity, we also need to normalize it so that its integral over the entire physical space is unity. More details concerning the mathematical background necessary to introduce Eq. (9) can be found in Davit and Quintard (2015) and Quintard and Whitaker (1994a,b). In order to construct an intrinsic phase average, we further define the β-phase volume fraction at point $\mathbf{x}$ by

$$\alpha_\beta = g * \gamma_\beta = \int_{\mathbb{R}^d} g(\mathbf{x}-\mathbf{r})\gamma_\beta(\mathbf{r})\,\mathrm{d}\mathbf{r} \tag{10}$$

where γ_β is the β-phase indicator function, whose value is 1 if $\mathbf{x}$ is located in the β-phase and 0 otherwise. The intrinsic phase

average of ψ_β is defined as

$$\langle\psi_\beta\rangle^\beta = \frac{g*\psi_\beta}{g*\gamma_\beta} = \frac{\langle\psi_\beta\rangle}{\alpha_\beta} \tag{11}$$

Second, we now average the micro-scale heat Eq. (5) on the averaging volume $\mathcal{V}$, by multiplying the micro-scale transport Eq. (5) by $\gamma_\beta g(\mathbf{x}-\mathbf{r})$, and then integrating it over the physical space to finally apply the general transport theorem (Whitaker, 1985), which leads to

$$\partial_t\left((\rho c_p)_\beta\langle T_\beta\rangle\right) + \nabla\cdot\langle(\rho c_p)_\beta T_\beta\mathbf{u}_\beta\rangle = \nabla\cdot\langle\lambda_\beta\nabla T_\beta\rangle + \langle\mathbf{n}_{\beta\sigma}\cdot\lambda_\beta\nabla T_\beta\delta_{\beta\sigma}\rangle \tag{12}$$

where $\delta_{\beta\sigma}$ is the Dirac delta function associated to the interface between the two phases.

Next, we introduce the perturbation decomposition of ψ_β into an average and a deviation $\widetilde{\psi}_\beta$ (see for instance Gray, 1975)

$$\psi_\beta = \langle\psi_\beta\rangle^\beta + \widetilde{\psi}_\beta \tag{13}$$

Finally, following Carbonell and Whitaker (1984), Gray (1975) and Quintard and Whitaker (1993a), we write the averaged equation, Eq. (12), as

$$\begin{aligned}\partial_t\left(\alpha_\beta(\rho c_p)_\beta\langle T_\beta\rangle^\beta\right) &+ \nabla\cdot\left(\alpha_\beta(\rho c_p)_\beta\langle T_\beta\rangle^\beta\langle\mathbf{u}_\beta\rangle^\beta\right)\\ &= \nabla\cdot\left(\alpha_\beta\lambda_\beta\nabla\langle T_\beta\rangle^\beta + \langle\lambda_\beta\widetilde{T}_\beta\mathbf{n}_{\beta\sigma}\delta_{\beta\sigma}\rangle\right)\\ &- \nabla\alpha_\beta\cdot\lambda_\beta\nabla\langle T_\beta\rangle^\beta + \langle\mathbf{n}_{\beta\sigma}\cdot\lambda_\beta\nabla\widetilde{T}_\beta\delta_{\beta\sigma}\rangle\\ &- \nabla\cdot\left((\rho c_p)_\beta\langle\widetilde{T}_\beta\widetilde{\mathbf{u}}_\beta\rangle^\beta\right)\end{aligned} \tag{14}$$

where we have ignored the variations of the physical properties within the averaging volume.

The Lagrangian description of the dispersed phase is obtained by integrating the micro-scale heat transfer Eq. (8) over each particle (Crowe et al., 2011). The boundary condition Eq. (6) leads to the following equation for the averaged particle temperature T_p

$$(mc_p)_p\frac{dT_p}{dt} = \int_{A_p}\mathbf{n}\cdot\lambda_\beta\nabla T_\beta\,\mathrm{d}S + \omega_p V_p \tag{15}$$

where V_p is the volume of the particle. At this stage of the developments, we have obtained the macro-scale Euler–Lagrange description that corresponds to Eqs. (14) and (15) of the heat transfer problem. However, they are not in a closed form since the temperature deviations $\widetilde{T}_\beta$ are still present. To get rid of these deviations, it is necessary to propose an estimation of the deviation from its boundary value problem. In order to obtain the governing equation for the deviation $\widetilde{T}_\beta$, we introduce the decomposition Eq. (13) in the micro-scale Eq. (5), and then we subtract the averaged Eq. (14) divided by α_β. The micro-scale transport equation for the deviation may be written as

$$\begin{aligned}(\rho c_p)_\beta\partial_t\widetilde{T}_\beta &+ (\rho c_p)_\beta\mathbf{u}_\beta\cdot\nabla\widetilde{T}_\beta + (\rho c_p)_\beta\widetilde{\mathbf{u}}_\beta\cdot\nabla\langle T_\beta\rangle^\beta\\ &= \nabla\cdot\left(\lambda_\beta\nabla\widetilde{T}_\beta\right) - \alpha_\beta^{-1}\nabla\cdot\langle\lambda_\beta\widetilde{T}_\beta\mathbf{n}_{\beta\sigma}\delta_{\beta\sigma}\rangle\\ &- \alpha_\beta^{-1}\langle\mathbf{n}_{\beta\sigma}\cdot\lambda_\beta\nabla\widetilde{T}_\beta\delta_{\beta\sigma}\rangle + \alpha_\beta^{-1}\nabla\cdot\left((\rho c_p)_\beta\langle\widetilde{T}_\beta\widetilde{\mathbf{u}}_\beta\rangle\right)\end{aligned} \tag{16}$$

The corresponding boundary conditions are also obtained by introducing the decomposition Eq. (13) in the boundary conditions Eqs. (6) and (7). As a result, one obtains the following set of boundary conditions on each particle surface A_p, $1\le p\le N_\mathcal{V}$

$$\widetilde{T}_\beta = T_\sigma - \langle T_\beta\rangle^\beta \tag{17}$$

$$\lambda_\beta\nabla\widetilde{T}_\beta\cdot\mathbf{n}_{\beta\sigma} = \left(\lambda_\sigma\nabla T_\sigma - \lambda_\beta\nabla\langle T_\beta\rangle^\beta\right)\cdot\mathbf{n}_{\beta\sigma} \tag{18}$$

These equations can be simplified through an evaluation of the orders of magnitude of the different terms. Introducing the decomposition Eq. (13) in the boundary conditions (7) and in the no-slip condition ($\mathbf{u}_\beta = 0$) at the $\beta-\sigma$ interface leads to an estimation of the order of magnitude of the velocity deviation $\widetilde{\mathbf{u}}_\beta$ and of $\widetilde{T}_\beta$ as (see Carbonell and Whitaker, 1984; Quintard and Whitaker, 1993a; Quintard and Whitaker, 2000)

$$\widetilde{\mathbf{u}}_\beta = \mathcal{O}\left(\langle\mathbf{u}_\beta\rangle^\beta\right) \tag{19}$$

$$\widetilde{T}_\beta = \mathcal{O}\left(\frac{l_\beta}{L_\beta}\langle T_\beta\rangle^\beta\right) \tag{20}$$

Furthermore, according to the developments in Quintard and Whitaker (1993a,b), the specific area can be estimated by

$$\langle\mathbf{n}_{\beta\sigma}\gamma_\beta\delta_{\beta\sigma}\rangle = \frac{A_{\beta\sigma}}{\mathcal{V}} = \mathcal{O}\left(\frac{\alpha_\beta}{l_\beta}\right) \tag{21}$$

where l_β is the micro-scale characteristic length. Eqs. (19)–(21) allow us to obtain the following estimates

$$\lambda_\beta\nabla^2\widetilde{T}_\beta = \mathcal{O}\left(\frac{\lambda_\beta}{l_\beta L_\beta}\langle T_\beta\rangle^\beta\right) \tag{22}$$

$$\alpha_\beta^{-1}\nabla\cdot\langle\lambda_\beta\widetilde{T}_\beta\mathbf{n}_{\beta\sigma}\delta_{\beta\sigma}\rangle = \mathcal{O}\left(\frac{\lambda_\beta}{L_\beta^2}\langle T_\beta\rangle^\beta\right) \tag{23}$$

$$\alpha_\beta^{-1}\nabla\cdot\left(\alpha_\beta(\rho c_p)_\beta\langle\widetilde{T}_\beta\widetilde{\mathbf{u}}_\beta\rangle\right) = \mathcal{O}\left(\left(\rho_\beta c_p\right)_\beta\frac{l_\beta}{L_\beta^2}\langle T_\beta\rangle^\beta\langle\mathbf{u}_\beta\rangle^\beta\right) \tag{24}$$

$$\left(\rho_\beta c_p\right)_\beta\mathbf{u}_\beta\cdot\nabla\widetilde{T}_\beta = \mathcal{O}\left(\left(\rho_\beta c_p\right)_\beta\frac{1}{L_\beta}\langle T_\beta\rangle^\beta\langle\mathbf{u}_\beta\rangle^\beta\right) \tag{25}$$

Using the length-scale constraint $l_\beta \ll L_\beta$ further leads to

$$\alpha_\beta^{-1}\nabla\cdot\langle\lambda_\beta\widetilde{T}_\beta\mathbf{n}_{\beta\sigma}\delta_{\beta\sigma}\rangle \ll \lambda_\beta\nabla^2\widetilde{T}_\beta \tag{26}$$

$$\alpha_\beta^{-1}\nabla\cdot\left(\alpha_\beta(\rho c_p)_\beta\langle\widetilde{T}_\beta\widetilde{\mathbf{u}}_\beta\rangle\right) \ll \left(\rho_\beta c_p\right)_\beta\mathbf{u}_\beta\cdot\nabla\widetilde{T}_\beta \tag{27}$$

Therefore, the micro-scale transport equation for the deviation Eq. (16) can be rewritten as

$$\begin{aligned}(\rho c_p)_\beta\partial_t\widetilde{T}_\beta &+ (\rho c_p)_\beta\mathbf{u}_\beta\cdot\nabla\widetilde{T}_\beta + (\rho c_p)_\beta\widetilde{\mathbf{u}}_\beta\cdot\nabla\langle T_\beta\rangle^\beta\\ &= \nabla\cdot\left(\lambda_\beta\nabla\widetilde{T}_\beta\right) - \alpha_\beta^{-1}\langle\mathbf{n}_{\beta\sigma}\cdot\lambda_\beta\nabla\widetilde{T}_\beta\delta_{\beta\sigma}\rangle\end{aligned} \tag{28}$$

As previously discussed, the thermal conductivity in the solid, λ_σ, is much larger than the thermal conductivity in the β-phase and thus the boundary condition Eq. (6) yields

$$|\nabla T_\sigma| = \left|\frac{\lambda_\beta}{\lambda_\sigma}\nabla T_\beta\right| \ll |\nabla T_\beta| \tag{29}$$

This implies that the temperature field can be considered uniform within each particle and that the boundary condition Eq. (18) can be eliminated from the micro-scale boundary value problem for the deviation while boundary condition Eq. (17) reads

$$\widetilde{T}_\beta = T_p - \langle T_\beta\rangle^\beta \quad \text{at } A_p\,,\ 1\le p\le N_\mathcal{V} \tag{30}$$

One way to proceed further would be to solve simultaneously the macroscopic problem and the problem for the deviation $\widetilde{T}_\beta$, which in many ways is more complex than solving the initial one Eqs. (5)–(8). There is another way to proceed that consists in building an approximate form of the deviations $\widetilde{T}_\beta$ by mapping it to macroscopic quantities through closure variables. As we will see, this makes it possible to fully uncouple micro- and macro-scale problems.

3.2. Unsteady closure

In the boundary value problem for the deviation Eqs. (17)–(28), we can identify the macroscopic quantities $(T_p - \langle T_\beta\rangle^\beta|_{\mathbf{x}_p})$ with

$1 \leq p \leq N_\mathcal{V}$ and $\nabla\langle T_\beta\rangle^\beta$. These terms can be treated as macroscopic source terms responsible for generating the spatial deviation $\widetilde{T}_\beta$. In this way, deviations can be mapped to these source terms (Carbonell and Whitaker, 1984; Quintard et al., 1997; Quintard and Whitaker, 1993a; 2000; Zanotti and Carbonell, 1984) through closure variables.

To build the form of a local solution for the spatial deviation, we first follow Davit and Quintard (2012) and Moyne (1997) to express the deviation in the form of a time convolution according to

$$\widetilde{T}_\beta = -\sum_{p=1}^{N_\mathcal{V}} s_p * \partial_t\left(\langle T_\beta\rangle^\beta|_{\mathbf{x}_p} - T_p\right) + \mathbf{b}_\beta \cdot * \partial_t \nabla\langle T_\beta\rangle^\beta \tag{31}$$

where s_p and $\mathbf{b}_\beta$ are the closure variables, which depend on space $\mathbf{x}$ and time t. The time convolution, denoted here by $*$, is defined for the functions a and b as

$$(a * b)(t) = \int_0^t a(t-\tau)b(\tau)\,\mathrm{d}\tau \tag{32}$$

The closure variables are solutions of unsteady closure problems given in Appendix A.2, in which we have assumed thermal equilibrium at $t<0$. These closure problems need to be solved in geometries representative of the structure of interest and, in many cases, this is done in unit cells with periodic boundary conditions. Effects of using periodic unit cells on the macroscopic results and the validity of the method in ordered and disordered systems are further discussed in Quintard et al. (1997) and Quintard and Whitaker (1993a). For disordered media, the periodicity conditions can be used when the size of the unit cell is sufficiently large compared to the correlation lengths of the heterogeneities (Quintard et al., 1997).

For the Eulerian field, we inject Eq. (31) in the averaged transport Eq. (14) and obtain

$$\begin{aligned}\partial_t\left(\alpha_\beta(\rho c_p)_\beta\langle T_\beta\rangle^\beta\right) + \nabla\cdot\left(\alpha_\beta(\rho c_p)_\beta\langle T_\beta\rangle^\beta\langle\mathbf{u}_\beta\rangle^\beta\right)\\ = \nabla\cdot\left(\mathbf{K}_{\beta\beta}\cdot *\partial_t\left(\nabla\langle T_\beta\rangle^\beta\right)\right) - \sum_{p=1}^{N} g(\mathbf{x}-\mathbf{x}_p)Q_{\beta p}\\ + \sum_{p=1}^{N}\nabla\cdot\left(\mathbf{d}_{\beta p} * \partial_t\left(\langle T_\beta\rangle^\beta|_{\mathbf{x}_p} - T_p\right)\right)\end{aligned} \tag{33}$$

where $\mathbf{K}_{\beta\beta}$ is the effective thermal dispersion defined by Eq. (121) and accounts for thermal conduction, tortuosity and hydrodynamic thermal dispersion. The coefficient $\mathbf{d}_{\beta p}$ is an additional velocity-like coefficient and is defined by Eq. (122). Finally, $Q_{\beta p}$ represents the macro-scale heat transfer between the continuous phase and the particle p and is defined by

$$\begin{aligned}Q_{\beta p} = \int_{A_p}\mathbf{n}\cdot\lambda_\beta\nabla\langle T_\beta\rangle^\beta\,\mathrm{d}S + A_p\sum_{k=1}^{N_\mathcal{V}} h_{pk} * \partial_t\left(\langle T_\beta\rangle^\beta|_{\mathbf{x}_k} - T_k\right)\\ - \mathbf{v}_{\beta p}\cdot *\partial_t\left(\nabla\langle T_\beta\rangle^\beta\right)\end{aligned} \tag{34}$$

The effective properties h_{pk} defined by Eq. (93) and $\mathbf{v}_{\beta p}$ defined by Eq. (98) are respectively the effective heat exchange coefficients and the velocity-like coefficient.

For the Lagrangian description of the dispersed phase, substituting Eq. (31) into Eq. (15) and using the definition Eq. (34) of the macro-scale heat transfer yields for averaged particle temperature T_p

$$(mc_p)_p\frac{dT_p}{dt} = Q_{\beta p} + \omega_p V_p \tag{35}$$

In these macro-scale Euler–Lagrange equations, both the thermal dispersion tensor, $\mathbf{K}_{\beta\beta}$, and the heat exchange coefficients, h_{pk}, appearing in Eqs. (33)–(35) look like classical terms. This contrasts with the velocity-like $\mathbf{v}_{\beta p}$ and additional velocity-like $\mathbf{d}_{\beta p}$ terms that do not appear in the classical macro-scale Euler–Lagrange description (Crowe et al., 2011; Ling et al., 2016; Michaelides and Feng, 1994; Simonin, 1996; Zhang and Prosperetti, 1997). These can be calculated from the closure problems given in Appendix A.2 and their contributions have been studied in the literature (Quintard et al., 1997; Zhang and Huang, 2001) for heat transfer in porous media with a thermal non-equilibrium model. In this work, we assume that the contributions of the non-classical terms can be neglected compared to the classical terms. In doing so, we obtain the following simplified model

$$\begin{aligned}\partial_t\left(\alpha_\beta(\rho c_p)_\beta\langle T_\beta\rangle^\beta\right) + \nabla\cdot\left(\alpha_\beta(\rho c_p)_\beta\langle T_\beta\rangle^\beta\langle\mathbf{u}_\beta\rangle^\beta\right)\\ = \nabla\cdot\left(\mathbf{K}_{\beta\beta}\cdot *\partial_t\left(\nabla\langle T_\beta\rangle^\beta\right)\right) - \sum_{p=1}^{N_\mathcal{V}} g(\mathbf{x}-\mathbf{x}_p)Q_{\beta p}\end{aligned} \tag{36}$$

$$(mc_p)_p\frac{dT_p}{dt} = Q_{\beta p} + \omega_p V_p \tag{37}$$

where

$$Q_{\beta p} = \int_{A_p}\mathbf{n}\cdot\lambda_\beta\nabla\langle T_\beta\rangle^\beta\,\mathrm{d}S + A_p\sum_{k=1}^{N_\mathcal{V}} h_{pk} * \partial_t\left(\langle T_\beta\rangle^\beta|_{\mathbf{x}_k} - T_k\right) \tag{38}$$

3.3. Steady-state closure

Eqs. (36)–(38) are obtained by expressing the spatial deviation in the form of a time convolution. The main consequence is that the resulting effective transport coefficients in the model are not only depending on the physical properties and the micro-scale geometry but they also depend upon time. In addition, the macro-scale Euler–Lagrange equations with unsteady closure problems must degenerate into the quasi-steady version when the macroscopic time is significantly greater than the characteristic time associated to the relaxation of the micro-scale conduction process (Davit and Quintard, 2012; Moyne, 1997). This constraint has been discussed in previous works (Quintard et al., 1997; Quintard and Whitaker, 1993a) and can be written as

$$\frac{\lambda_\beta t}{(\rho c_p)_\beta l_\beta^2} \gg 1 \tag{39}$$

When this is verified, the unsteady term in the transport equation for $\widetilde{T}_\beta$ can be neglected, so that the boundary value problem for the deviation can be treated as quasi-steady. Following previous works Carbonell and Whitaker (1984), Quintard et al. (1997) and Quintard and Whitaker (1993a, 2000), we can then express the deviation in terms of the macroscopic source terms as

$$\widetilde{T}_\beta = -\sum_{p=1}^{N_\mathcal{V}} s_p^\infty\left(\langle T_\beta\rangle^\beta|_{\mathbf{x}_p} - T_p\right) + \mathbf{b}_\beta^\infty\cdot\nabla\langle T_\beta\rangle^\beta \tag{40}$$

Here, the mapping variables s_p^∞ and $\mathbf{b}_\beta^\infty$ are solutions of the quasi-steady problems given in Appendix A.2. This asymptotic behavior corresponds to the transition form s_p and $\mathbf{b}_\beta$ to the limit $u(t)s_p^\infty$ and $u(t)\mathbf{b}_\beta^\infty$ in the convolution product defined by Eq. (31), where $u(t)$ is the Heaviside function. These decompositions can be written as follows (Davit and Quintard, 2012)

$$s_p - u(t)s_p^\infty = s_p^* \tag{41}$$

$$\mathbf{b}_\beta - u(t)\mathbf{b}_\beta^\infty = \mathbf{b}_\beta^* \tag{42}$$

where s_p^* and $\mathbf{b}_\beta^*$ represent the contribution of history effects in the unsteady closure problem and verify respectively

$$\lim_{t\to+\infty} s_p^* = 0, \text{ and } \lim_{t\to+\infty}\mathbf{b}_\beta^* = 0 \tag{43}$$

The mapping variables associated with the history effects s_p^* and $\mathbf{b}_\beta^*$ are solutions of the closure problems related to the history effects (Appendix A.3). These closure problems are obtained by introducing the decompositions Eqs. (41) and (42) into the unsteady closure problems (Appendix A.1), then subtracting the quasi-stationary closure problems (Appendix A.2) multiplied by $u(t)$.

Similarly, introducing the decompositions Eqs. (41) and (42) respectively in Eqs. (93) and (121) yields the following expression for the effective transport coefficients h_{pk} and $\mathbf{K}_{\beta\beta}$

$$h_{pk} = u(t)h_{pk}^{\infty} + h_{pk}^{*} \tag{44}$$

$$\mathbf{K}_{\beta\beta} = u(t)\mathbf{K}_{\beta\beta}^{\infty} + \mathbf{K}_{\beta\beta}^{*} \tag{45}$$

where h_{pk}^* and $\mathbf{K}_{\beta\beta}^*$ are respectively the effective heat exchange and the effective thermal dispersion coefficients related to history effects. The definitions of these coefficients are given in appendix Eqs. (115)–(125).

Lastly, by introducing Eqs. (44) and (45) into the averaged transport equation for the β-phase Eq. (36) and the equation for the averaged particle temperature Eq. (38), the macro-scale Euler–Lagrange equations with unsteady closure problems can be written as

$$\begin{aligned}\partial_t\left(\alpha_\beta(\rho c_p)_\beta\langle T_\beta\rangle^\beta\right) + \nabla\cdot\left(\alpha_\beta(\rho c_p)_\beta\langle T_\beta\rangle^\beta\langle\mathbf{u}_\beta\rangle^\beta\right)\\ = \nabla\cdot\left(\mathbf{K}_{\beta\beta}^{\infty}\cdot\nabla\langle T_\beta\rangle^\beta\right) - \sum_{p=1}^{N_\mathcal{V}} g(\mathbf{x}-\mathbf{x}_p)Q_{\beta p}\\ + \nabla\cdot\left(\mathbf{K}_{\beta\beta}^{*}\cdot *\partial_t\left(\nabla\langle T_\beta\rangle^\beta\right)\right)\end{aligned} \tag{46}$$

$$(mc_p)_p\frac{dT_p}{dt} = Q_{\beta p} + \omega_p V_p \tag{47}$$

where

$$\begin{aligned}Q_{\beta p} = \int_{A_p}\mathbf{n}\cdot\lambda_\beta\nabla\langle T_\beta\rangle^\beta\,\mathrm{d}S + A_p\sum_{k=1}^{N_\mathcal{V}} h_{pk}^{\infty}\left(\langle T_\beta\rangle^\beta|_{\mathbf{x}_k} - T_k\right)\\ + A_p\sum_{k=1}^{N_\mathcal{V}} h_{pk}^{*} * \partial_t\left(\langle T_\beta\rangle^\beta|_{\mathbf{x}_k} - T_k\right)\end{aligned} \tag{48}$$

In the averaged transport equation for the β-phase Eq. (46), the first term corresponds to the quasi-steady conductive term; the second term to the macro-scale heat transfer between the continuous phase and particles in the averaging volume; and the last term takes the form of a history integral that accounts for memory effects of the unsteady thermal conduction. The appearance of this term is a direct consequence of the decomposition in the quasi-steady and memory contributions of the effective thermal dispersion.

In the macro-scale heat exchange Eq. (48), the first term looks like, at least formally, the undisturbed heat flux contribution while the second term corresponds to the quasi-steady thermal transfer from the particle to the continuous phase. The last term represents the unsteady thermal diffusion due to the temporal variation of the thermal boundary layer around the particles in the averaging volume. This contribution accounts for the effect of the past history temperature changes of the β-phase and particles within the averaging volume to the current temperature change of the pth-particle.

4. Theoretical comparison with standard models

When comparing the classical Euler–Lagrange model with the proposed model (46)–(48), the main differences are the convolution term in Eq. (46) and the expression of the macro-scale heat exchange term $Q_{\beta p}$. In this section, we review these differences in detail for the cases of isolated particles and clouds of particles.

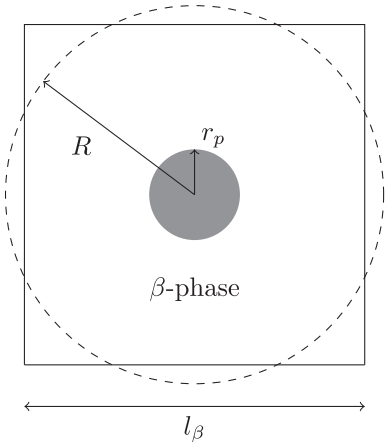

Fig. 2. Comparison of Chang's unit cell (dashed line) with a spatially periodic system (solid line).

4.1. Isolated particle

As mentioned in the introduction, the modeling of heat exchange between the filtered continuous phase and the particles is usually based on the description of heat transfer for an isolated particle in an infinite medium (Crowe et al., 2011; Ling et al., 2016; Michaelides and Feng, 1994; Zhang and Prosperetti, 1997). This description uses a decomposition of the surrounding β-phase temperature into an undisturbed thermal field T_β^0, which is not influenced by the presence of the particle, and a disturbance field, which is entirely due to the influence of the heat transfer from the particle.

In order to compare our model to the standard results in the case of an isolated particle, we consider the case of a single isolated spherical particle with no macroscopic gradient. We consider an immobile sphere in a spherical unit cell, as represented in Fig. 2, which is a spherical version of Chang's unit cell (Chang, 1983). This unit cell has been extensively studied in the literature (Quintard and Whitaker, 1993b; 1995) as it allows to obtain an analytical solution of the closure problems. Following Quintard and Whitaker (1995), the correspondence between the Chang's unit cell and the spatially periodic system is obtained by requiring that the volume fraction be equal. This leads to $l_\beta^3 = (4/3)\pi R^3$ where R is the radius of the Chang's unit cell illustrated in Fig. 2. The radius of the particle, r_p, and the characteristic length of the unit cell, R, are linked by

$$R = \frac{r_p}{\left(1-\alpha_\beta\right)^{1/3}} \tag{49}$$

The closure problem associated to Chang's unit cell for the mapping variable s_p^∞ can be written as

$$0 = \lambda_\beta\nabla^2 s_p^\infty - \alpha_\beta^{-1}\frac{A_p}{\mathcal{V}}h_p^\infty\,, \quad \text{for } r_p \le r \le R \tag{50}$$

$$s_p^\infty = 1\,, \quad \text{at } r = r_p \tag{51}$$

$$\mathbf{n}\cdot\nabla s_p^\infty = 0\,, \quad \text{at } r = R \tag{52}$$

$$\text{Average: } \langle s_p^\infty\rangle^\beta = 0 \tag{53}$$

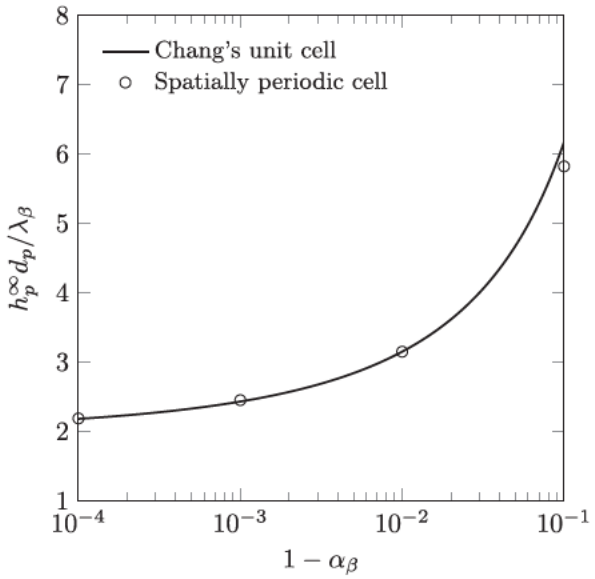

Fig. 3. Dimensionless heat transfer coefficient as a function of the solid volume fraction for the Chang's unit cell and the spatially periodic system.

where h_p^∞ refers here to h_{pp}^∞ (single particle within the representative unit cell) and is given by

$$h_p^\infty = -\frac{1}{A_p}\int_{A_p} \mathbf{n}\cdot\lambda_\beta\nabla s_p^\infty \,\mathrm{d}S \tag{54}$$

To solve analytically the closure problem, we proceed as follows. First, the exchange coefficient h_p^∞ is treated as an unknown constant and the problem given by Eqs. (50)–(52) is solved. We thus obtain the mapping variable s_p^∞ as a function of the exchange coefficient. As a second step, the average constraint Eq. (53) is used to determine the exchange coefficient. Following this methodology, the quasi-steady exchange coefficient can be written as

$$\frac{h_p^\infty d_p}{\lambda_\beta} = \frac{10\alpha_\beta^2}{9\left(1-\left(1-\alpha_\beta\right)^{\frac{1}{3}}\right)-\alpha_\beta\left(3+\alpha_\beta\right)} \tag{55}$$

For an isolated particle in an infinite continuous phase ($\alpha_\beta \to 1$), h_p^∞ reduces to the classical quasi-steady heat exchange coefficient (Michaelides and Feng, 1994)

$$\lim_{\alpha_\beta\to 1}\frac{h_p^\infty d_p}{\lambda_\beta} = 2 \tag{56}$$

The correspondence between the Chang's unit cell and the spatially periodic system has been studied elsewhere (Quintard and Whitaker, 1993b; 1995) and we just repeat here the analysis performed in Quintard and Whitaker (1995) by comparing the analytical solution and the numerical solution of the closure problem for the spatially periodic system. Results displayed in Fig. 3 are in accordance with previous results reported in Quintard and Whitaker (1995) and show a very good agreement between the analytical solution and the numerical one, at least for low values of the solid volume fraction α_σ, which correspond here to the domain of interest.

Moving to the unsteady closure problem, in order to solve analytically the closure problem, we further use a Laplace transform to eliminate the convolutions. The unilateral Laplace transform is defined by

$$\overline{\psi} = \int_0^\infty e^{-\xi t}\psi \,\mathrm{d}t \tag{57}$$

where ξ is the Laplace variable. Applying the Laplace transform to the closure problem associated with Chang's unit cell for the mapping variable s_p^* yields to the following problem for $\overline{s}_p^*$

$$\left(\rho_\beta c_p\right)_\beta\left(\xi\overline{s}_p^* + s_p^\infty\right) = \lambda_\beta\nabla^2\overline{s}_p^* - \alpha_\beta^{-1}\frac{A_p}{\mathcal{V}}\overline{h}_p^*, \quad \text{for } r_p \le r \le R \tag{58}$$

$$\overline{s}_p^* = 0, \quad \text{at } r = r_p \tag{59}$$

$$\mathbf{n}\cdot\nabla\overline{s}_p^* = 0, \quad \text{at } r = R \tag{60}$$

$$\text{Average: } \langle\overline{s}_p^*\rangle^\beta = 0 \tag{61}$$

with

$$\overline{h}_p^* = -\frac{1}{A_p}\int_{A_p}\mathbf{n}\cdot\lambda_\beta\nabla\overline{s}_p^*\,\mathrm{d}S \tag{62}$$

This problem can be solved analytically with the same methodology outlined for the quasi-steady case. The coefficient $\overline{h}_p^*$ has been obtained in the Laplace domain as a function of α_β as well as the physical properties. Unfortunately $\overline{h}_p^*$ is a complex expression and the analytical expression of h_p^* cannot be given in the time domain. As a consequence, the constraint $\alpha_\beta \to 1$ is directly introduced into the expression of $\overline{h}_p^*$, which leads to

$$\lim_{\alpha_\beta\to 1}\overline{h}_p^* = \lambda_\beta\sqrt{\frac{(\rho c_p)_\beta}{\lambda_\beta\xi}} \tag{63}$$

Applying the inverse Laplace transform to h_p^* leads to the classical kernel used for the unsteady heat exchange for an isolated particle in an infinite continuous phase (Michaelides and Feng, 1994)

$$h_p^* = \lambda_\beta\left(\frac{\lambda_\beta}{(\rho c_p)_\beta}\pi t\right)^{-1/2} \tag{64}$$

Introducing Eqs. (56) and (64) into Eqs. (47) and (48) leads to the classical energy equation of a rigid sphere in a continuous phase (Michaelides and Feng, 1994)

$$(mc_p)_p\frac{dT_p}{dt} = 2\pi\lambda_\beta d_p\left(\langle T_\beta\rangle^\beta|_{\mathbf{x}_p} - T_p\right) + \pi\lambda_\beta d_p^2\int_0^t \frac{\dfrac{d\left(\langle T_\beta\rangle^\beta|_{\mathbf{x}_p} - T_p\right)}{d\tau}}{\left(\dfrac{\lambda_\beta}{\left(\rho_\beta c_p\right)_\beta}\pi\left(t-\tau\right)\right)^{1/2}}\,\mathrm{d}\tau \tag{65}$$

Due to this specific configuration, the contribution involving the macroscopic β-phase temperature gradient that usually refers to the undisturbed heat flux seen by the particle is absent from the energy equation. Besides the fact that the temperatures are spatial averages, we recover known results in the case of an isolated particles including history effects.

4.2. Cloud of particles

The case of a cloud of particles is fundamentally different. For a cloud containing N_p particles, the fluid temperature T_β^0 seen by the pth-particle is that locally undisturbed by the presence of particle p, but taking into account the disturbance created by all other $N_p - 1$ particles in the cloud (Boivin et al., 1998). Restricting to very diluted cases when α_β is very close to one, perturbations to the temperature field induced by the presence of other particles can be neglected and this leads to the one-way coupling

(Crowe et al., 2011) for which T_β^0 is identical to the fluid temperature without particles. Moving to less dilute cases that lead to the two-way coupling (Crowe et al., 2011), the locally undisturbed fluid temperature is usually treated as a macro-scale temperature $\langle T_\beta \rangle^\beta$ provided that the characteristic lengthscale r_g is much larger than the particle diameter (Boivin et al., 1998; Climent and Magnaudet, 2006). In this work, the use of spatial averaging with closure follows similar constraints but allows us to obtain an expression of the heat exchange that is much more general. This is because the temperature in the β-phase is decomposed into the averaged temperature $\langle T_\beta \rangle^\beta$ and a deviation, without assuming that the particle is isolated. The result is an expression for the deviation that takes into account the effects of all the $N_\mathcal{V}$ particles within the averaging volume. The heat exchange for the pth-particle explicitly captures the effects of other particles as well as the pth-particle and the Euler–Lagrange equations, Eqs. (46)–(48), are a generalization of the classical models (Crowe et al., 2011; Ling et al., 2016; Michaelides and Feng, 1994; Zhang and Prosperetti, 1997). This generalization degenerates toward the standard models when the exchange between the filtered continuous phase and the pth-particle is the dominant contribution in the heat exchange $Q_{\beta p}$. In this case, we can diagonalize the heat exchange matrix and obtain

$$Q_{\beta p} = \int_{A_p} \mathbf{n} \cdot \lambda_\beta \nabla \langle T_\beta \rangle^\beta \, \mathrm{d}S + A_p h_p^\infty \left(\langle T_\beta \rangle^\beta |_{\mathbf{x}_p} - T_p \right) + A_p h_p^* * \partial_t \left(\langle T_\beta \rangle^\beta |_{\mathbf{x}_p} - T_p \right) \tag{66}$$

where h_p^∞ and h_p^* are obtained by solving the closure problems for unit cell with isolated particle.

It is also of some interest to perform a preliminary comparison between the proposed macro-scale description and heat transfer models that take into account some particle–particle interactions on average in the frame of Eulerian–Eulerian descriptions. For small Reynolds numbers, spatially periodic models of the micro-scale geometry usually leads to good estimates of the effective transport coefficients (Carbonell and Whitaker, 1984) while higher Reynolds number flow cases require more realistic configurations such that the ones carried out in Sun et al. (2015) and Thiam et al. (2019). Hence, restricting to small Reynolds numbers, it can be instructive to compare the analytical result obtained for the Chang's unit cell with heat transfer models used in Eulerian–Eulerian descriptions (Gunn, 1978; Sun et al., 2015). This can be achieved by first establishing a correspondence between Eulerian–Eulerian and Eulerian–Lagrangian descriptions that reads here for the average temperature of the dispersed phase in the simple case of monodisperse spherical particles

$$\langle T_\sigma \rangle^\sigma = \frac{1}{N_\mathcal{V}} \sum_{p=1}^{N_\mathcal{V}} T_p \tag{67}$$

For motionless particles in a quiescent continuous phase and restricting further to the case where there is no averaged temperature gradient and to the quasi-steady closure, the resulting macro-scale description reads

$$\alpha_\beta (\rho c_p)_\beta \frac{d\langle T_\beta \rangle^\beta}{dt} = -a_v h_p^\infty \left(\langle T_\beta \rangle^\beta - \langle T_\sigma \rangle^\sigma \right) \tag{68}$$

$$\alpha_\sigma (\rho c_p)_\sigma \frac{d\langle T_\sigma \rangle^\sigma}{dt} = -a_v h_p^\infty \left(\langle T_\sigma \rangle^\sigma - \langle T_\beta \rangle^\beta \right) + \frac{1}{\mathcal{V}} \sum_{p=1}^{N_\mathcal{V}} \omega_p V_p \tag{69}$$

where $a_v = N_\mathcal{V} A_p / \mathcal{V}$ denotes the interfacial area per unit volume and h_p^∞ corresponds to lumped coefficients

$$h_p^\infty = \sum_{k=1}^{N_\mathcal{V}} h_{pk}^\infty \tag{70}$$

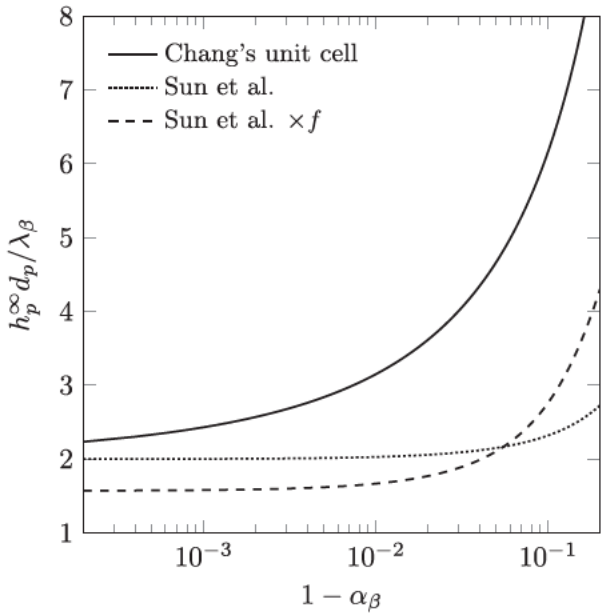

Fig. 4. Dimensionless heat transfer coefficient as a function of the solid volume fraction for the Chang's unit cell and the correlations proposed by Sun et al. (2015) at vanishing Reynolds number.

Hence, the analytical estimate Eq. (55) obtained from the Chang's unit cell can be compared with empirical correlations for some average Nussel number $\langle \mathrm{Nu} \rangle$. Using the Gunn's correlation (Gunn, 1978) that has been established for a wide range of volume fraction and restricting to vanishing Reynolds numbers, we follow here Sun et al. (2015) to express the average Nusselt number as

$$\langle \mathrm{Nu} \rangle = \left(7 - 10\alpha_\beta + 5\alpha_\beta^2\right) f^{-1}(\alpha_\beta), \qquad f(\alpha_\beta) = \frac{4}{\pi}\left(1 - 1.6\alpha_\sigma\alpha_\beta - 3\alpha_\sigma\alpha_\beta^4\right) \tag{71}$$

where $f(\alpha_\beta)$ is a correction factor that relates the Nusselt number based on the continuous phase temperature to the one based on the bulk temperature (Sun et al., 2015; Thiam et al., 2019). A comparison between the above correlation and the estimate provided by Eq. (55) for the Chang's unit cell is reported in Fig. 4. Despite the simplicity of the Chang's unit cell, the analytical estimate follows similar tendencies featured by empirical correlations. While such an estimate is expected to over-predict heat transfers for moderate to high values of the solid volume fraction (Quintard and Whitaker, 1995), it fulfills the correct asymptotic behavior for very low solid volume fraction contrary to correlations that use the correction factor that tend to under-predict heat transfers in this dilute regime (Thiam et al., 2019).

5. Results for model cloud cases

The main purpose of this section is to study our model and compare it to standard approaches in idealized cloud configurations. Such model cloud cases allow us to get a reference solution by solving numerically the micro-scale heat transfer problem and averaging the obtained results for the micro-scale temperature fields T_β and T_σ. We focus on systems that are infinite in all directions and where there is no average temperature gradient in Eqs. (46)–(48). We further study a relatively dilute dispersed two-phase flow in the laminar regime with particles smaller than 10^{-4} m. The velocity of the continuous phase is considered uniform and the relative velocity between the particles and the continuous phase is neglected. Positioning the coordinate system in a moving

frame attached to the continuous phase allows us to further remove the convective term in Eq. (46) and the undisturbed heat flow in Eq. (48).

In this case, the macroscopic description is a 0D problem with

$$\alpha_\beta(\rho c_p)_\beta \frac{d\langle T_\beta\rangle^\beta}{dt} = -\frac{1}{\mathcal{V}}\sum_{p=1}^{N_\mathcal{V}} Q_{\beta p} \tag{72}$$

$$(mc_p)_p \frac{dT_p}{dt} = Q_{\beta p} + \omega_p V_p \tag{73}$$

where

$$Q_{\beta p} = \sum_{k=1}^{N_\mathcal{V}} A_p h^\infty_{pk}\left(\langle T_\beta\rangle^\beta|_{\mathbf{x}_k} - T_k\right) + \sum_{k=1}^{N_\mathcal{V}} A_p h^*_{pk} * \partial_t\left(\langle T_\beta\rangle^\beta|_{\mathbf{x}_k} - T_k\right) \tag{74}$$

Here, we have used the classical box weighting function g defined by

$$g(\mathbf{x}) = \begin{cases} \dfrac{1}{\mathcal{V}}, & \mathbf{x}\in\mathcal{V} \\ 0, & \mathbf{x}\notin\mathcal{V} \end{cases} \tag{75}$$

In this framework with no average gradient, only the closure problems for s^∞_p and s^*_p need to be solved.

As stated previously, the accuracy of the macro-scale models is assessed by comparing results to computations of the complete micro-scale problem. In the remainder of this section, these micro-scale simulations are termed Direct Numerical Simulations (DNS). We consider two different studies. In the first study, the validity of both the unsteady and quasi-steady models is addressed for a micro-scale one-dimensional geometry for which the closure problems as well as the macroscopic equations can be solved analytically. In the second study, we consider only the quasi-steady approximation and we assess the validity of a diagonal approximation of the heat exchange matrix for two- and three-dimensional geometries. DNS of the micro-scale problem have been performed using the CALIF^{3}S software (CALIF) that employs unstructured finite volume discretization. The interested reader is referred to Piar et al. (2013) for a detailed presentation of the finite volume discretization based on the SUSHI scheme for the approximation of the diffusive fluxes.

5.1. Validity of the quasi-steady closure

In this section, we compare the unsteady and quasi-steady models. The micro-scale structure is a one-dimensional geometry illustrated in Fig. 5 and consists in an array of three particles with the same diameter d_p and separated by the distance l_β.

The averaging volume is assumed to be spatially periodic (Davit and Quintard, 2015; Quintard and Whitaker, 1993a). Further, taking into account the symmetry with respect to the center of particle 1, the matrix of heat exchange coefficients is symmetric $h^\infty_{pk} = h^\infty_{kp}$. Moreover the considered geometry allows us to solve analytically the coefficients and to determine them all from only h^∞_{11} and h^∞_{12} (see Appendix C.1).

The macro-scale Eulerian–Lagrangian ordinary differential equations are non-dimensionalized with the following dimensionless variables

$$\hat\nabla = l_\beta\nabla\ ;\ \hat t = \frac{\lambda_\beta}{l^2_\beta(\rho c_p)_\beta}t\ ;\ \hat\omega_p = \frac{l^2_\beta}{T_r\lambda_\beta\varphi}\omega_p\ ;$$
$$\varphi = \frac{(\rho c_p)_p}{(\rho c_p)_\beta}\ ;\ \hat h^\infty_{pk} = \frac{l^2_\beta A_p}{\lambda_\beta\mathcal{V}}h^\infty_{pk}\ ;\ \hat T_\eta = \frac{T_\eta - T_r}{T_r},\ \text{with } \eta = \beta, k \tag{76}$$

where T_r refers to some reference temperature. The corresponding macro-scale equations can be expressed in matrix form according to

$$\frac{d}{d\hat t}[\hat T] = \mathcal{H}^\infty\cdot[\hat T] + [\hat\omega] \tag{77}$$

where $[\hat T]$ and $[\hat\omega]$ are column vectors and $\mathcal{H}^\infty$ is a four-by-four matrix. All three can be represented explicitly as

$$[\hat T] = \begin{pmatrix} \langle\hat T_\beta\rangle^\beta \\ \hat T_1 \\ \hat T_2 \\ \hat T_{2'} \end{pmatrix}\ ;\ [\hat\omega] = \begin{pmatrix} 0 \\ \hat\omega_1 \\ \hat\omega_2 \\ \hat\omega_{2'} \end{pmatrix} \tag{78}$$

$$\mathcal{H}^\infty = \frac{3}{\alpha_\sigma\varphi}\begin{pmatrix} -\frac{\alpha_\sigma\varphi}{\alpha_\beta}\hat h^\infty & \frac{\alpha_\sigma\varphi}{3\alpha_\beta}\hat h^\infty & \frac{\alpha_\sigma\varphi}{3\alpha_\beta}\hat h^\infty & \frac{\alpha_\sigma\varphi}{3\alpha_\beta}\hat h^\infty \\ \hat h^\infty & -\hat h^\infty_{11} & -\hat h^\infty_{12} & -\hat h^\infty_{12} \\ \hat h^\infty & -\hat h^\infty_{12} & -\hat h^\infty_{11} & -\hat h^\infty_{12} \\ \hat h^\infty & -\hat h^\infty_{12} & -\hat h^\infty_{12} & -\hat h^\infty_{11} \end{pmatrix} \tag{79}$$

where $\hat h^\infty = \hat h^\infty_{11} + 2\hat h^\infty_{12}$.

By using the matrix exponential $\exp(.)$ (see e.g., Magnus, 1954), the solution of the linear differential equation system Eq. (77) is given by

$$[\hat T](\hat t) = \left(\int_0^{\hat t}\exp\left(u\mathcal{H}^\infty\right)\mathrm{d}u\right)\cdot[\hat\omega] + e^{\hat t\mathcal{H}^\infty}\cdot[\hat T_0] \tag{80}$$

where the vector $[\hat T_0]$ represents the vector $[\hat T]$ at the initial state. The matrix $\mathcal{H}^\infty$ is diagonalizable with three distinct eigenvalues a_0, a_1 and a_2 defined by

$$\{a_0, a_1, a_2\} = \left\{0, -\frac{3\left(\hat h^\infty_{11} - \hat h^\infty_{12}\right)}{\alpha_\sigma\varphi}, -3\hat h^\infty\left(\frac{1}{\alpha_\sigma\varphi} + \frac{1}{\alpha_\beta}\right)\right\} \tag{81}$$

We apply successively the Cayley–Hamilton theorem and Sylvester's formula to $\exp(u\mathcal{H}^\infty)$ (for example, see Horn and Johnson, 1990; Cvetkovic et al., 1997). Accordingly, Eq. (80) reads

$$[\hat T](\hat t) = \mathcal{F}_0\cdot[\hat T_0] - \sum_{i=1}^{2}\frac{1}{a_i}\mathcal{F}_i\cdot[\hat\omega] + \mathcal{F}_0\cdot[\hat\omega]\hat t + \sum_{i=1}^{2}e^{a_i\hat t}\mathcal{F}_i\cdot\left(\frac{1}{a_i}[\hat\omega] + [\hat T_0]\right) \tag{82}$$

where $\mathcal{F}_i$ are the Frobenius covariants of the matrix $\mathcal{H}^\infty$, defined by

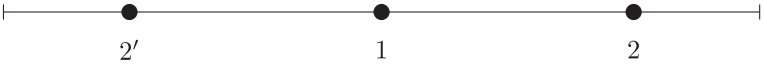

Fig. 5. Micro-scale one-dimensional system with $N_\mathcal{V} = 3$.

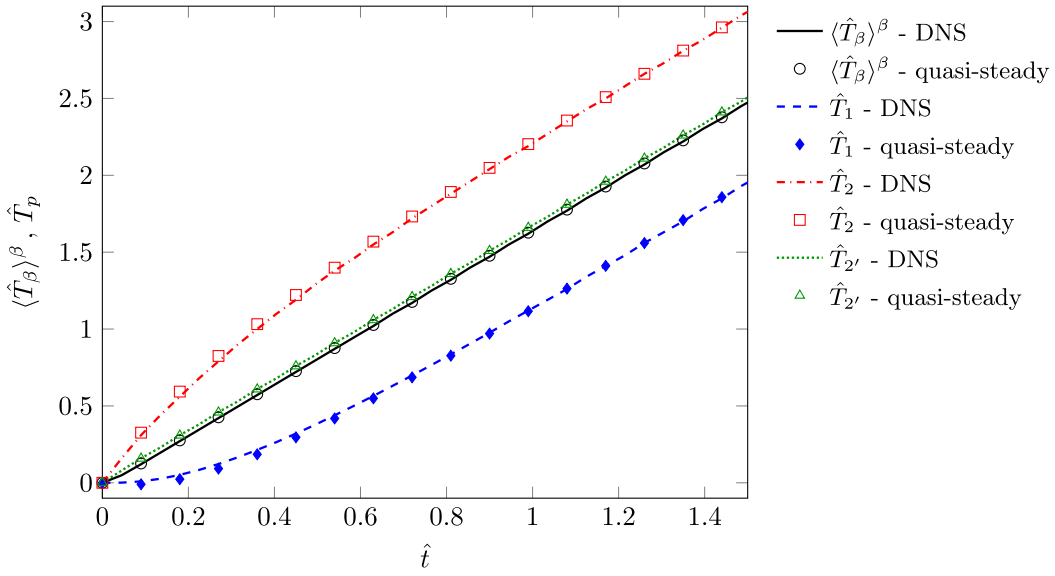

Fig. 6. Comparison of the quasi-steady closure with the reference solution obtained by averaging Direct Numerical Simulations (DNS) results of the micro-scale problem.

Table 1
Model parameters.

Parameter	$\frac{\lambda_\sigma}{\lambda_\beta}$	$\frac{(\rho c_p)_\sigma}{(\rho c_p)_\beta}$	α_σ	T_r	$\hat{\omega}_1$	$\hat{\omega}_2$	$\hat{\omega}_{2'}$
Value	10^3	10^3	10^{-3}	300	0	10	5

$$\mathcal{F}_i = \prod_{i=0,\ j\neq i}^{2} \frac{1}{a_i - a_j}\left(\mathcal{H}^\infty - a_j \mathcal{I}\right) \tag{83}$$

where $\mathcal{I}$ is the identity matrix.

The micro-scale problem, Eqs. (5)–(8), is solved numerically to obtain the T_β and T_σ fields, which can be averaged to produce the reference values for the macro-scale models. Comparisons are carried out for scenarios of dust explosion typical of nuclear safety (Table 1). Results in Fig. 6 show that the values obtained by the Euler–Lagrange model with the quasi-steady closure are in very good agreement with the reference values, particularly for a time greater than 0.5. For shorter times (*i.e.* $\hat{t} < 0.5$), a good agreement between results is observed for the averaged β-phase temperature, as well as the temperature of particles 2 and 2′. However, the temperature of the inert particle (particle 1) decreases initially and this is in clear contradiction with the micro-scale results Fig. 6 and in violation of physical principles.

To determine the origin of this difference and whether it is a consequence of the quasi-steady closure, we now consider the solution of the problem with history effects and compare the reference solution, the quasi-steady model and the fully transient formulations. The closure problems for the memory variable are solved analytically in the Laplace domain (Appendix C.2) and the Eulerian–Lagrangian model with the unsteady closure is rewritten in the Laplace domain as

$$\xi[\overline{\hat{T}}] - [\hat{T}_0] = \left(\overline{\mathcal{H}}^\infty + \xi \overline{\mathcal{H}}^*\right) \cdot [\overline{\hat{T}}] + [\overline{\hat{\omega}}] \tag{84}$$

where the overbar denotes the transformed variable in the Laplace domain. $\mathcal{H}^*$ is defined by analogy to the matrix $\mathcal{H}^\infty$ using the memory heat exchange coefficients. The solution of the system of linear equations (84) is straightforward and the temperatures in physical space are obtained by using numerical inverse Laplace algorithms. Results in Fig. 7 show that the model with the unsteady closure is in perfect agreement with the reference solution. The averaged temperatures are also very close to the two previous results if $\hat{t} < 0.5$ and the three types of results are similar for $\hat{t} > 0.5$.

This comparison demonstrates that our models accurately predict the averaged temperatures, even in the short-time limit. The quasi-steady assumption is valid when the constraint Eq. (39) is verified, which means that the history effects can be neglected. In the next study case, we consider only the quasi-steady model and assume that this constraint is verified.

5.2. Validity of the diagonalization for the heat exchange coefficients matrix

We now assess the accuracy of the quasi-steady macro-scale model for a two-dimensional micro-scale geometry and the impact of a diagonal approximation of the heat exchange coefficients matrix Eq. (79). Such a diagonalization consists in neglecting the indirect exchange between particles in Eqs. (72)–(74). To clarify this point, consider the following expression of the heat exchange

$$Q_{\beta p} = A_p h_p^\infty \left(\langle T_\beta \rangle^\beta|_{\mathbf{x}_p} - T_p\right) + \sum_{k=1}^{N_\gamma} A_p h_{pk}^\infty (T_p - T_k) \tag{85}$$

where h_p^∞ correspond to lumped coefficients already defined and that are recalled below

$$h_p^\infty = \sum_{k=1}^{N_\gamma} h_{pk}^\infty \tag{86}$$

Note that this expression is only valid when there is no averaged temperature gradient, thus allowing us to identify the macro-scale continuous phase temperature $\langle T_\beta \rangle^\beta|_{\mathbf{x}_k}$ with $\langle T_\beta \rangle^\beta|_{\mathbf{x}_p}$. The most straightforward way to obtain a diagonal approximation is therefore to neglect the sum in Eq. (85), which is often referred to as lumping the coefficients in the matrix. When this is done, the diagonal coefficients can be calculated from a single closure problem corresponding to the sum of all mapping variables (see Appendix D). This greatly simplifies the determination of the heat exchange coefficients and allows us to obtain analytical expressions for simple unit cells like the one illustrated in Fig. 2.

For instance, the lumped coefficients can be solved analytically for the cylindrical version of the Chang's unit cell shown in Fig. 2. As for the spherical case, we compare the analytical solution obtained for Chang's unit cell with the numerical solution of the

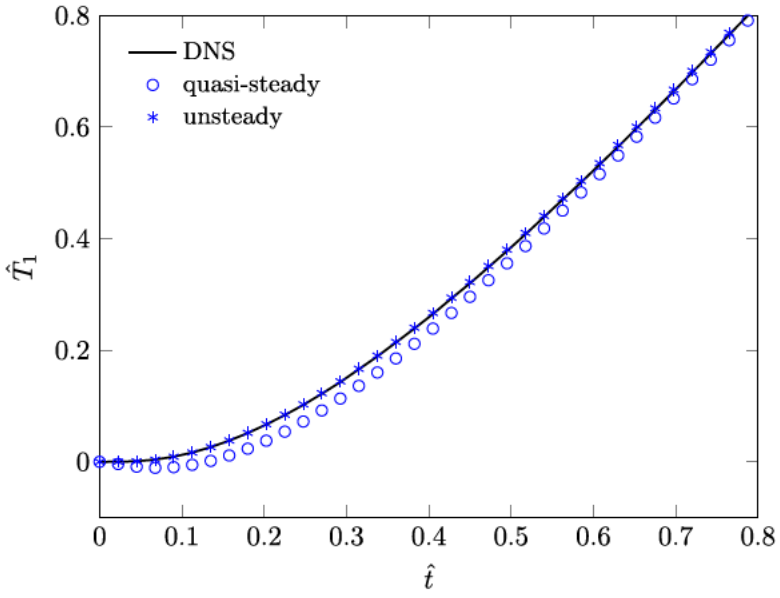

Fig. 7. Comparison between the unsteady/quasi-steady models and the reference solution obtained by averaging Direct Numerical Simulations (DNS) results of the micro-scale problem.

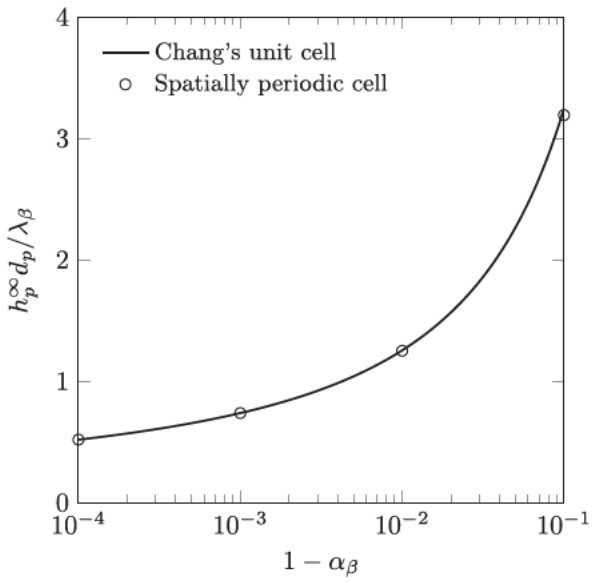

Fig. 8. Dimensionless heat transfer coefficient as a function of the solid volume fraction for the cylindrical version of the Chang's unit cell and the spatially periodic system.

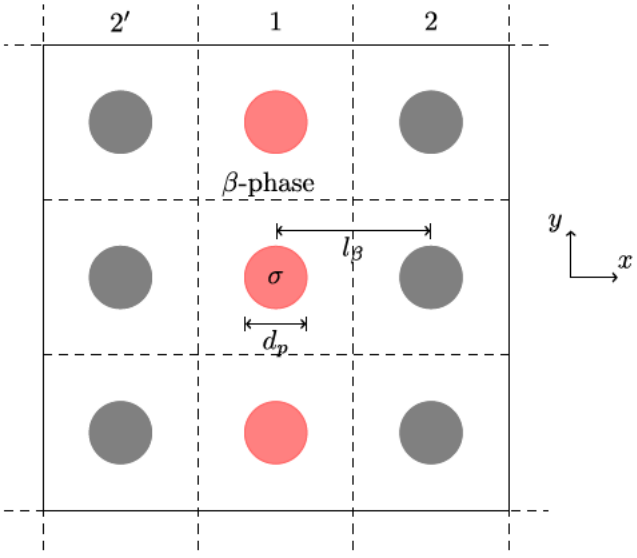

Fig. 9. Micro-scale two-dimensional geometry with $N_y = 3 \times 3$ particles.

closure problems for various volume fractions. Here again, the correspondence between the two cells requires that their volume fraction are identical (Quintard and Whitaker, 1995) and this leads to $\pi R^2 = l_\beta^2$, where R is the radius of the Chang's unit cell. The resulting lumped heat exchange coefficient reads

$$\frac{h_p^\infty d_p}{\lambda_\beta} = -\frac{8\alpha_\beta^2}{\alpha_\beta(2+\alpha_\beta)+2\log(1-\alpha_\beta)} \tag{87}$$

Results in Fig. 8 show a good agreement between the analytical solution and the numerical one as already observed in the spherical case and in Quintard and Whitaker (1995) for the cylindrical case for low values of α_σ, which is here the domain of interest.

The validity of the lumped approximation is tested for the two-dimensional system illustrated in Fig. 9. The micro-structure corresponds to a periodic arrangement of in-line cylinders that play the role of particles. Here again, there is no averaged temperature gradient and it is further assumed that the system is homogeneous in the y-direction. As a result, a single row of particles, as shown in Fig. 9, is representative of the entire system. Since we are interested in dilute gas-particle mixtures, we consider that the solid volume fraction α_σ should remain below 10^{-3}. Using this upper bound, the value of the heat exchange coefficients are reported in Table 2. The first line with $N_y = 1$ corresponds to the previously discussed spatially periodic cell in connection with the Chang's unit cell. The second line with $N_y = 3$ corresponds to the case of interest. The results for N_y up to 13 particles within the averaging volume are reported in Table 2. They show that the value of the lumped coefficient h_p^∞ is much larger than the value of h_{pk}^∞

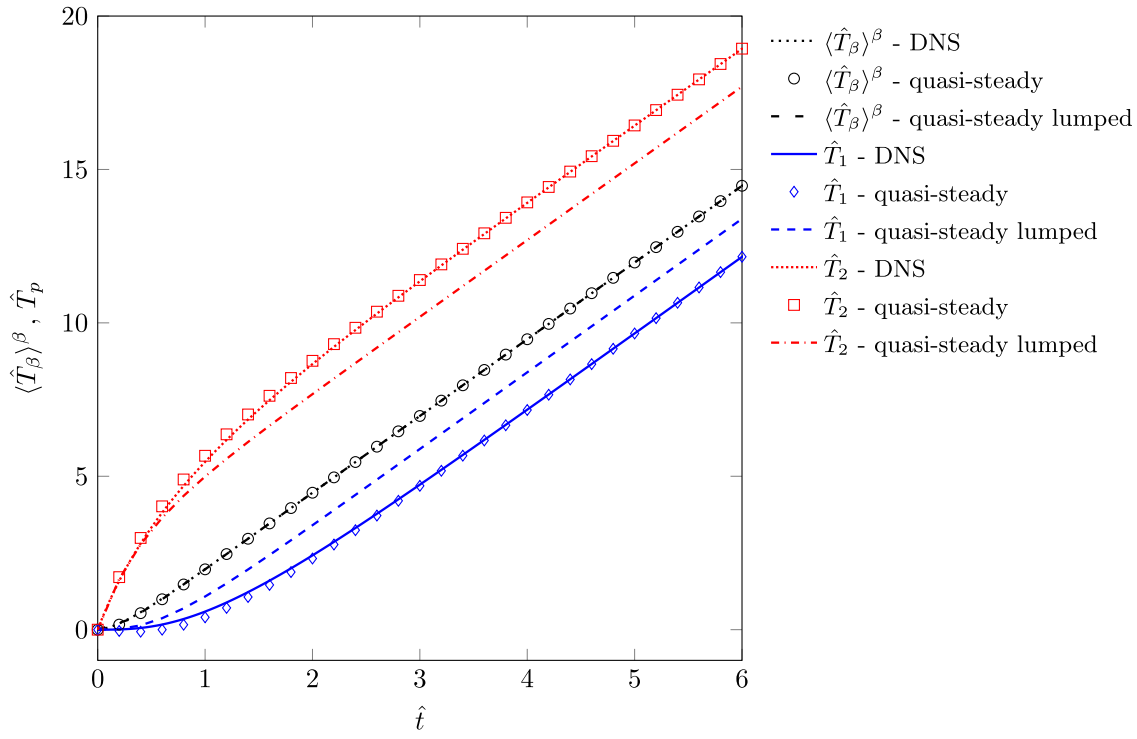

Fig. 10. Comparison of averaged DNS results with the macro-scale predictions for both the quasi-steady and the quasi-steady lumped approximation – two-dimensional case $N_\mathcal{V} = 3 \times 3$.

Table 2
Dimensionless heat exchange coefficients $\hat{h}_{pk} = h^\infty_{pk} d_p/\lambda_\beta$ for different values of $N_\mathcal{V}$ and $\alpha_\sigma = 10^{-3}$ for a periodic arrangement of in-line cylinders ($\parallel$ denotes particles on the same x-axis, $\perp$ between the first and the second rows and $\perp\perp$ between the first and the third rows).

$N_\mathcal{V}$	$\hat{h}_{11}$	$\hat{h}_{12\parallel}$	$\hat{h}_{12\perp}$	$\hat{h}_{13\parallel}$	$\hat{h}_{13\perp}$	$\hat{h}_{13\perp\perp}$
1	0.737					
3×3	0.537	0.01	0.039			
5×5	0.492	−0.028	0.0017	0.0186	0.0218	0.025

except for the diagonal coefficient h^∞_{pp} which is of the same order of magnitude. Also note that the value of h^∞_p does not depend on $N_\mathcal{V}$ since the lumped coefficients can be obtained from summing mapping variables s defined in Appendix D and solved for the spatially periodic cell shown in Fig. 8.

Next, we compare the average temperature $\langle T_\beta \rangle^\beta$ and the temperatures of particles 1, 2 and 2′ obtained from micro-scale simulations to those obtained from the macro-scale Eulerian–Lagrangian description using the heat exchange coefficients given in Table 2 and the same parameter values reported in Table 1. Recall from Eq. (85) that the lumped approximation is formally equivalent to the full macro-scale heat exchange coefficients matrix when there is no temperature difference between particles. The proposed case involving active and inert particles leads to large temperature differences between particles and, therefore, allows us to test the validity of the lumped approximation. Parameters are listed in Table 1 and results are plotted in Fig. 10. We find that the quasi-steady model is in good agreement with the reference micro-scale simulations for a dimensionless time greater than 3 (recall that the theoretical constraint is $\hat{t} \gg 1$).

The lumped approximation yields a good agreement for the averaged β-phase temperature $\langle T_\beta \rangle^\beta$ but an underestimation of the temperature difference between particles. In order to get more insight for larger temperature differences between particles, we extend the previous case to $N_\mathcal{V} = 5$ with only particle 1 remaining active and $\hat{\omega}_1 = 100$. The results reported in Fig. 11 show that the lumped approximation still yields a good agreement for $\langle T_\beta \rangle^\beta$ at $\hat{t} > 4$ but fails to capture differences observed in DNS results for particles 1 and 3.

We further remark that other diagonal approximations may produce better results. In this specific configuration, Fig. 12 shows that we obtain slightly better results if we substitute the lumped coefficients by the diagonal coefficients h^∞_{pp} reported in Table 2. This suggests that, depending on the situation of interest, different diagonalizations may yield better results. This is something that needs to be addressed in future works, especially when considering average gradients of temperature.

We move finally to the three-dimensional case and assess the validity of the lumped approximation for the three-dimensional version of the system illustrated in Fig. 9 that consists in a periodic arrangement of in-line spherical particles. As previously, it is assumed that there is no averaged temperature gradient and that the system is homogeneous except in the x-direction. As a result, here again a single row of particles along the x-direction is representative of the entire system. We do not repeat here all the cases studied previously in the two-dimensional case and we restrict to the case $N_\mathcal{V} = 3 \times 3 \times 3$. The results reported in Fig. 13 in which the β-phase average temperature $\langle T_\beta \rangle^\beta$ is compared to the temperatures of particles reflect the same trends as already observed in the previous two-dimensional case. Here again, the quasi-steady approximation leads to a good prediction of the macro-scale temperatures while the lumped approximation fails to accurately predict the temperatures of particles. It is instructive to note that in this special case of ordered distribution of spherical particles with large temperature difference between particles and with no averaged temperature gradient in the continuous phase, both the quasi-steady and the quasi-steady lumped approximation yields

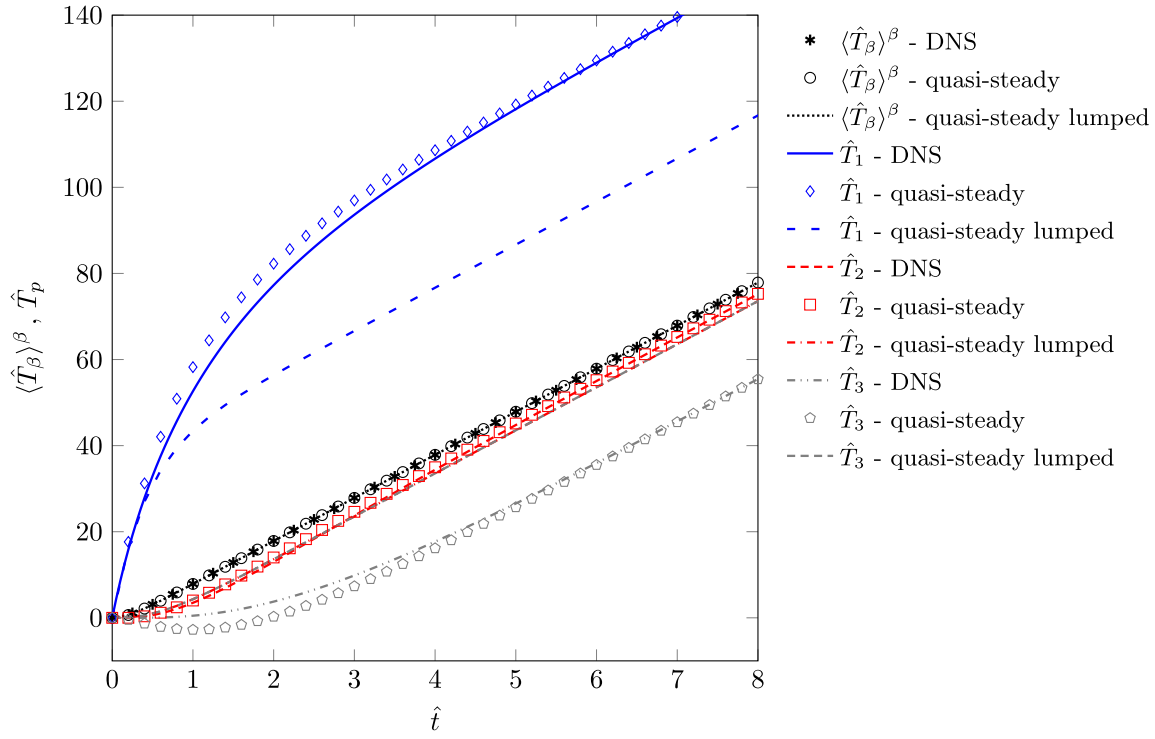

Fig. 11. Comparison of averaged DNS results with the macro-scale predictions for both quasi-steady and quasi-steady lumped approximations – two-dimensional case $N_\nu = 5 \times 5$.

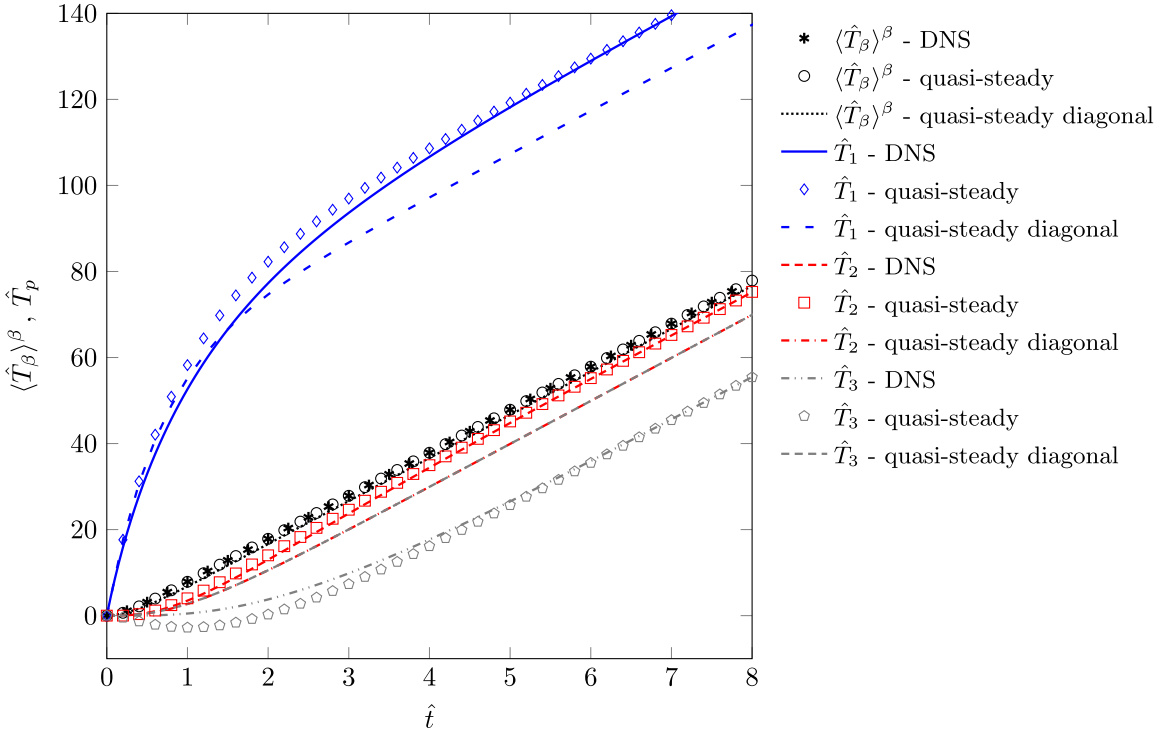

Fig. 12. Comparison of averaged DNS results with the macro-scale predictions for both quasi-steady and quasi-steady diagonal approximations – two-dimensional case $N_\nu = 5 \times 5$.

the same averaged temperature for the continuous phase. This behavior was expected from Eqs. (68) to (69) as macro-scale Eulerian description is equivalent to the lumped approximation. This also means that in this case, the lumped approximation accurately predict the averaged temperature for the dispersed phase defined by Eq. (67).

6. Discussion and conclusion

Using the method of volume averaging with closure, we have derived a novel macroscopic Euler–Lagrange model for heat transfer in gas-particle mixtures. The primary difference between our model and the classical one is an expression of heat

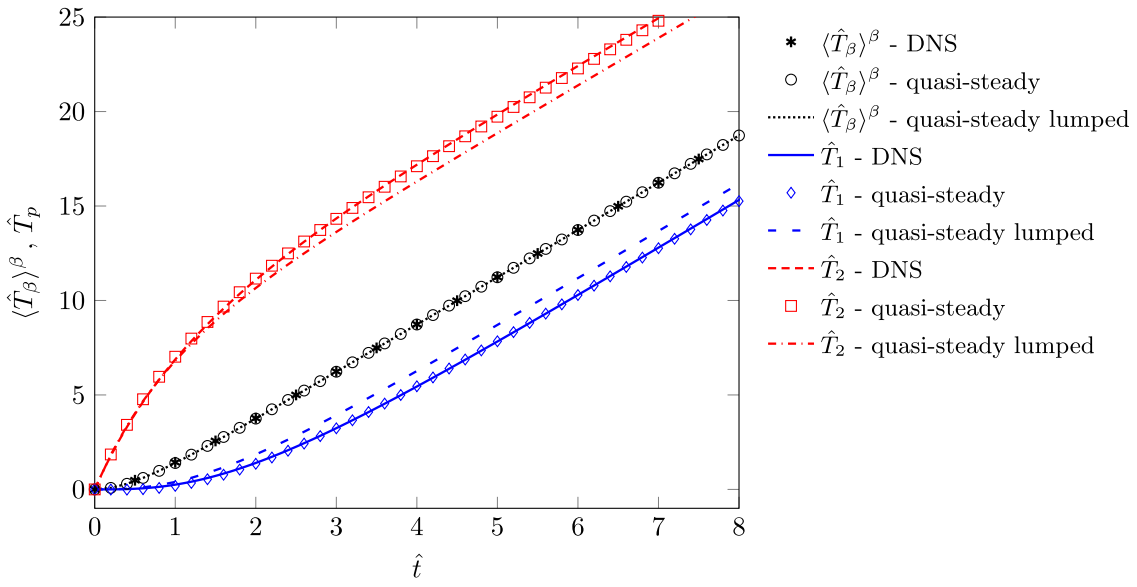

Fig. 13. Comparison of averaged DNS results with the macro-scale predictions for both the quasi-steady and the quasi-steady lumped approximation – three-dimensional case $N_\mathcal{V} = 3 \times 3 \times 3$.

transfers that captures indirect particle–particle interactions. We recall here that indirect exchanges refer to heat transfer between particles through the continuous carrier phase and have not to be confused with direct particle–particle exchanges that take place during collisions in dense suspensions. By comparing our theory to micro-scale computations in simple model cases of particle clouds, we found that the general formulation with time convolutions is able to predict the exact macroscopic temperatures for any time in a case with no average gradient. This shows that the most general formulation of the heat transfer captures both history effects and heat exchanges between particles. We have also shown that the quasi-steady model accurately captures the temperature fields for sufficiently long times. This illustrates the usefulness of the quasi-steady approximation which is, in practice, frequently adopted when the constraint Eq. (39) is verified.

We have further shown that the standard formulations can be recovered from a diagonalization approximation of the exchange matrix. In particular, a lumped matrix can be used and the diagonal coefficients can be obtained by solving the closure problem for a unit cell with an isolated particle, similarly to the classical approach. This approximation is formally equivalent to the full macro-scale model when the temperature differences between particles can be neglected. This approximation was tested in the case of two- and three-dimensional systems. The simplified version of the model was able to accurately describe the average temperature $\langle T_\beta \rangle^\beta$. However, the lumped approximation failed in capturing temperature differences between particles, which is due to the fact that the indirect exchange between the particles is neglected.

The considered model cases of particle clouds, even if very simple, have led us to a better fundamental understanding of the models. The validity of the various macro-scale approximations have been assessed in cases with large temperature difference between particles within the averaging volume but no average gradients of temperature. Therefore, limitations of the standard description, which neglect both indirect exchange between particles and memory effects, must be further evaluated in practical cases with macroscopic gradients.

Such practical cases would require more realistic configurations such as random arrangements of spherical particles investigated in Sun et al. (2015) and Thiam et al. (2019) for the closure of Eulerian–Eulerian heat transfer using direct numerical simulations. This would represent a highly challenging task since different arrangements that correspond to the same volume fraction may lead to very different heat transfer coefficients values. One could then adopt the methodology followed in the Eulerian–Eulerian framework by using ensemble average of a number of realizations to get relationships for the effective properties such as $h_{pk} = h_{pk}(\alpha_\beta)$. However, it is not clear at this stage on how this methodology may apply in the Eulerian–Lagrangian framework (Kriebitzsch et al., 2013) and this calls to future work.

Appendix A. Closure problems

In order to obtain the closure problems for the mappings variables, we introduce Eq. (40) in the local problem for the deviation $\widetilde{T}_\beta$ and proceed in the standard way in the volume averaging theory. In doing so, we obtain $N_\mathcal{V}$ identical closure problems I_k for the variables s_k and the closure problem II for variable $\mathbf{b}_\beta$. These problems are as follows.

A1. Unsteady closure problems

– Problem $\mathbf{I}_k$ for s_k with $1 \leq k \leq N_\mathcal{V}$

$$\left(\rho_\beta c_p\right)_\beta \left(\partial_t s_k + \mathbf{u}_\beta \cdot \nabla s_k\right) = \lambda_\beta \nabla^2 s_k - \alpha_\beta^{-1} \sum_{p=1}^{N_\mathcal{V}} g(\mathbf{x} - \mathbf{x}_p) A_p h_{pk}, \text{ in the } \beta\text{-phase} \tag{88}$$

$$s_k = 1, \text{ at } A_k \tag{89}$$

$$s_k = 0, \text{ at } A_j \text{ with } j \neq k \tag{90}$$

$$\text{Periodicity: } s_k(\mathbf{x} + \mathbf{r}) = s_k(\mathbf{x}) \tag{91}$$

$$\text{Initial condition: } s_k = 0, \text{ at } t = 0 \tag{92}$$

where:

$$h_{pk} = -\frac{1}{A_p} \int_{A_p} \mathbf{n} \cdot \lambda_\beta \nabla s_k \, \mathrm{d}S \tag{93}$$

– Problem II for $\mathbf{b}_\beta$

$$\left(\rho_\beta c_p\right)_\beta\left(\partial_t \mathbf{b}_\beta + \mathbf{u}_\beta \cdot \nabla \mathbf{b}_\beta + \mathbf{u}'_\beta\right) = \lambda_\beta \nabla^2 \mathbf{b}_\beta - \alpha_\beta^{-1} \sum_{k=1}^{N_\mathcal{V}} g(\mathbf{x}-\mathbf{x}_p)\mathbf{v}_{\beta p}, \text{ in the } \beta\text{-phase} \tag{94}$$

$$\mathbf{b}_\beta = 0, \text{ at } A_p, \text{ with } \ 1 \le p \le N_\mathcal{V} \tag{95}$$

$$\text{Periodicity: } \mathbf{b}_\beta(\mathbf{x}+\mathbf{r}) = \mathbf{b}_\beta(\mathbf{x}) \tag{96}$$

$$\text{Initial condition: } \mathbf{b}_\beta = 0, \text{ at } t = 0 \tag{97}$$

where:

$$\mathbf{v}_{\beta p}^\infty = \int_{A_p} \mathbf{n} \cdot \lambda_\beta \nabla \mathbf{b}_\beta \, \mathrm{d}S \tag{98}$$

A2. Quasi-steady closure problems

– Problem I_k^∞ for s_k^∞ with $1 \le k \le N_\mathcal{V}$

$$\left(\rho_\beta c_p\right)_\beta \mathbf{u}_\beta \cdot \nabla s_k^\infty = \lambda_\beta \nabla^2 s_k^\infty - \alpha_\beta^{-1} \sum_{p=1}^{N_\mathcal{V}} g(\mathbf{x}-\mathbf{x}_p) A_p h_{pk}^\infty, \text{ in the } \beta\text{-phase} \tag{99}$$

$$s_k^\infty = 1, \text{ at } A_k \tag{100}$$

$$s_k^\infty = 0, \text{ at } A_j \text{ with } j \ne k \tag{101}$$

$$\text{Periodicity: } s_k^\infty(\mathbf{x}+\mathbf{r}) = s_k^\infty(\mathbf{x}) \tag{102}$$

$$\text{Average: } \langle s_k^\infty \rangle^\beta = 0 \tag{103}$$

where:

$$h_{pk}^\infty = -\frac{1}{A_p} \int_{A_p} \mathbf{n} \cdot \lambda_\beta \nabla s_k^\infty \, \mathrm{d}S \tag{104}$$

– Problem II^∞ for $\mathbf{b}_\beta^\infty$

$$\left(\rho_\beta c_p\right)_\beta\left(\mathbf{u}_\beta \cdot \nabla \mathbf{b}_\beta^\infty + \mathbf{u}'_\beta\right) = \lambda_\beta \nabla^2 \mathbf{b}_\beta^\infty - \alpha_\beta^{-1} \sum_{p=1}^{N_\mathcal{V}} g(\mathbf{x}-\mathbf{x}_p)\mathbf{v}_{\beta p}^\infty, \text{ in the } \beta\text{-phase} \tag{105}$$

$$\mathbf{b}_\beta^\infty = 0, \text{ at } A_p, \text{ with } \ 1 \le p \le N_\mathcal{V} \tag{106}$$

$$\text{Periodicity: } \mathbf{b}_\beta^\infty(\mathbf{x}+\mathbf{r}) = \mathbf{b}_\beta^\infty(\mathbf{x}) \tag{107}$$

$$\text{Average: } \langle \mathbf{b}_\beta^\infty \rangle^\beta = 0 \tag{108}$$

where:

$$\mathbf{v}_{\beta p}^\infty = -\int_{A_p} \mathbf{n} \cdot \lambda_\beta \nabla \mathbf{b}_\beta^\infty \, \mathrm{d}S \tag{109}$$

A3. Memory effects closure problems

– Problem I_k^* for s_k^* with $1 \le k \le N_\mathcal{V}$

$$\left(\rho_\beta c_p\right)_\beta\left(\partial_t s_k^* + \mathbf{u}_\beta \cdot \nabla s_k^* + \delta(t) s_k^\infty\right) = \lambda_\beta \nabla^2 s_k^* - \alpha_\beta^{-1} \sum_{p=1}^{N_\mathcal{V}} g(\mathbf{x}-\mathbf{x}_p) A_p h_{pk}^*, \text{ in the } \beta\text{-phase} \tag{110}$$

$$s_k^* = 1 - u(t), \text{ at } A_k \tag{111}$$

$$s_k^* = 0, \text{ at } A_j \text{ with } j \ne k \tag{112}$$

$$\text{Periodicity: } s_k^*(\mathbf{x}+\mathbf{r}) = s_k^*(\mathbf{x}) \tag{113}$$

$$\text{Initial condition: } s_k^* = 0, \text{ at } t = 0 \tag{114}$$

where:

$$h_{pk}^* = -\frac{1}{A_p} \int_{A_p} \mathbf{n} \cdot \lambda_\beta \nabla s_k^* \, \mathrm{d}S \tag{115}$$

– Problem II^* for $\mathbf{b}_\beta^*$

$$\left(\rho_\beta c_p\right)_\beta\left(\partial_t \mathbf{b}_\beta^* + \mathbf{u}_\beta \cdot \nabla \mathbf{b}_\beta^* + \delta(t) s_j^\infty + (1-u(t))\mathbf{u}'_\beta\right) = \lambda_\beta \nabla^2 \mathbf{b}_\beta^* - \alpha_\beta^{-1} \sum_{p=1}^{N_\mathcal{V}} g(\mathbf{x}-\mathbf{x}_p)\mathbf{v}_{\beta p}^*, \text{ in the } \beta\text{-phase} \tag{116}$$

$$\mathbf{b}_\beta^* = 0, \text{ at } A_p, \ 1 \le p \le N_\mathcal{V} \tag{117}$$

$$\text{Periodicity: } \mathbf{b}_\beta^*(\mathbf{x}+\mathbf{r}) = \mathbf{b}_\beta^*(\mathbf{x}) \tag{118}$$

$$\text{Initial condition: } \mathbf{b}_\beta^* = 0, \text{ at } t = 0 \tag{119}$$

where:

$$\mathbf{v}_{\beta p}^* = -\int_{A_p} \mathbf{n} \cdot \lambda_\beta \nabla \mathbf{b}_\beta^* \, \mathrm{d}S \tag{120}$$

Appendix B. Definitions of the effective transport coefficients

$$\mathbf{K}_{\beta\beta} = \alpha_\beta \lambda_\beta \mathbf{I} + \langle \lambda_\beta \mathbf{n}_{\beta\sigma} \cdot \mathbf{b}_\beta \delta_{\beta\sigma} \rangle - (\rho c_p)_\beta \langle \mathbf{u}'_\beta \mathbf{b}_\beta \rangle \tag{121}$$

$$\mathbf{d}_{\beta p} = (\rho c_p)_\beta \langle s_p \mathbf{u}'_\beta \rangle - \langle \lambda_\beta s_p \mathbf{n}_{\beta\sigma} \delta_{\beta\sigma} \rangle \tag{122}$$

$$\mathbf{K}_{\beta\beta}^\infty = \alpha_\beta \lambda_\beta \mathbf{I} + \langle \lambda_\beta \mathbf{n}_{\beta\sigma} \cdot \mathbf{b}_\beta^\infty \delta_{\beta\sigma} \rangle - (\rho c_p)_\beta \langle \mathbf{u}'_\beta \mathbf{b}_\beta^\infty \rangle \tag{123}$$

$$\mathbf{d}_{\beta p}^\infty = (\rho c_p)_\beta \langle s_p^\infty \mathbf{u}'_\beta \rangle - \langle \lambda_\beta s_p^\infty \mathbf{n}_{\beta\sigma} \delta_{\beta\sigma} \rangle \tag{124}$$

$$\mathbf{K}_{\beta\beta}^* = \langle \lambda_\beta \mathbf{n}_{\beta\sigma} \cdot \mathbf{b}_\beta^* \delta_{\beta\sigma} \rangle - (\rho c_p)_\beta \langle \mathbf{u}'_\beta \mathbf{b}_\beta^* \rangle \tag{125}$$

$$\mathbf{d}_{\beta p}^* = \left(\rho_\beta c_p\right)_\beta \langle s_p^* \mathbf{u}'_\beta \rangle - \langle \lambda_\beta s_p^* \mathbf{n}_{\beta\sigma} \delta_{\beta\sigma} \rangle \tag{126}$$

Appendix C. Heat exchange coefficients for one-dimensional unit cells

C1. Quasi-steady closure problems

The closure problems I_k^∞ for the mapping variables s_k^∞ with $1 \le k \le N_\mathcal{V}$ read for one-dimensional unit cells as

$$0 = \frac{d^2 s_k^\infty}{dx'^2} - \alpha_\beta^{-1} \sum_{p=1}^{N_\mathcal{V}} \hat{h}_{pk}^\infty, \text{ in the } \beta\text{-phase} \tag{127}$$

$$s_k^\infty = 1, \text{ at } x' = x_k \pm r_k \tag{128}$$

$$s_k^\infty = 0, \text{ at } x' = x_p \pm r_p \text{ with } p \ne k \tag{129}$$

$$\text{Periodicity: } s_k^\infty(x'+L) = s_k^\infty(x') \tag{130}$$

$$\text{Average: } \langle s_k^\infty \rangle^\beta = 0 \tag{131}$$

where:

$$\hat{h}_{pk}^\infty = \frac{ds_k^\infty}{dx'}|_{(\mathbf{x}_p - r_p)} - \frac{ds_k^\infty}{dx'}|_{(\mathbf{x}_p + r_p)} \tag{132}$$

The solutions of the closure problems for s_k^∞ can be calculated from the second order polynomial for each interval $]x'_p; x'_{p+1}[$

$$s_k^\infty = \frac{1}{2}\alpha_\beta^{-1}\sum_{p=1}^{N_\mathcal{V}} \hat{h}_{pk}^\infty x'^2 + c_j x' + d_j \tag{133}$$

By introducing the previous expression into the closure problems, we obtain a linear system of 3×9 equations. The resolution of this system allows us to determine all the polynomial coefficients. Introducing the solution in Eq. (132) leads to

$$\hat{h}_{pk}^\infty = \begin{cases} \hat{h}_{11}^\infty ; & \text{if } p = k \\ \hat{h}_{12}^\infty ; & \text{if } p \neq k \end{cases} \tag{134}$$

where $\hat{h}_{11}^\infty$ and $\hat{h}_{12}^\infty$ are defined as

$$\hat{h}_{11}^\infty = \frac{6}{\alpha_\beta} - \frac{24\alpha_\beta^2}{36 - \alpha_\beta\big(38 - 3\big(1-\alpha_\beta\big)\alpha_\beta\big)} \tag{135}$$

$$\hat{h}_{12}^\infty = -\frac{3}{\alpha_\beta} - \frac{24\alpha_\beta^2}{36 - \alpha_\beta\big(38 - 3\big(1-\alpha_\beta\big)\alpha_\beta\big)} \tag{136}$$

C2. Memory effects closure problems

– Problem $\mathbf{I}_k^*$ for s_k^* with $1 \le k \le N_\mathcal{V}$

$$\partial_{t'} s_k^* + \delta(t') s_k^\infty = \nabla'^2 s_k^* - \alpha_\beta^{-1}\sum_{p=1}^{N_\mathcal{V}} \hat{h}_{pk}^*, \text{ in the } \beta\text{-phase} \tag{137}$$

$$s_k^* = 1 - u(t'), \text{ at } A_k \tag{138}$$

$$s_k^* = 0, \text{ at } A_j \text{ with } j \neq k \tag{139}$$

$$\text{Periodicity: } s_k^*(x' + L) = s_k^*(x') \tag{140}$$

$$\text{Initial condition: } s_k^* = 0, \text{ at } t' = 0 \tag{141}$$

where:

$$\hat{h}_{pk}^* = \partial_{x'} s_k^*|_{(\mathbf{x}_p - r_p)} - \partial_{x'} s_k^*|_{(\mathbf{x}_p + r_p)} \tag{142}$$

In Laplace space, the closure problem can be written as

$$\xi \bar{s}_k^* + s_k^\infty = \frac{d^2 \bar{s}_k^*}{x'^2} - \alpha_\beta^{-1}\sum_{p=1}^{N_\mathcal{V}} \bar{\hat{h}}_{pk}^*, \text{ in the } \beta\text{-phase} \tag{143}$$

$$\bar{s}_k^* = 0, \text{ at } A_p \text{ with } 1 \le p \le N_\mathcal{V} \tag{144}$$

$$\text{Periodicity: } \bar{s}_k^*(x' + L) = \bar{s}_k^*(x') \tag{145}$$

$$\text{Average: } \langle \bar{s}_k^* \rangle^\beta = 0 \tag{146}$$

where:

$$\hat{h}_{pk}^* = \frac{d\bar{s}_k^*}{dx'}|_{(\mathbf{x}_p - r_p)} - \frac{d\bar{s}_k^*}{dx'}|_{(\mathbf{x}_p + r_p)} \tag{147}$$

The solutions of those closure problems can be calculated from

$$\bar{s}_k^* = c_k e^{\sqrt{\xi}x'} + d_k e^{\sqrt{\xi}x'} - \frac{1}{\xi}\alpha_\beta^{-1}\sum_{p=1}^{N_\mathcal{V}} \bar{\hat{h}}_{pk}^* - \alpha_\beta^{-1}\left(\frac{1}{\xi^2} + \frac{x'^2}{2\xi}\right)\sum_{p=1}^{N_\mathcal{V}} \hat{h}_{pk}^\infty - \frac{c_k x' + d_k}{\xi} \tag{148}$$

Using the same methodology as in the previous section, the heat exchange coefficients $\bar{\hat{h}}_{pk}^*$ can be rewritten as

$$\bar{\hat{h}}_{pk}^* = \begin{cases} \bar{\hat{h}}_{11}^* ; & \text{if } p = k \\ \bar{\hat{h}}_{12}^* ; & \text{if } p \neq k \end{cases} \tag{149}$$

$$\bar{\hat{h}}_{11}^* = \frac{\alpha_\beta(3\coth(\kappa) + \tanh(\kappa))}{18\kappa} + \frac{2\alpha_\beta^4}{9(1-\kappa\coth(\kappa))f(\alpha_\beta)} - \frac{\alpha_\beta}{6\kappa^2 f(\alpha_\beta)}\big(36 - \alpha_\beta\big(38 - \big(3 - 7\alpha_\beta\big)\alpha_\beta\big)\big) \tag{150}$$

$$\bar{\hat{h}}_{12}^* = \frac{8\alpha_\beta^4 \kappa e^{-\kappa}}{36(\kappa-1)f(\alpha_\beta)(\kappa\cosh(\kappa) - \sinh(\kappa))} - \frac{\alpha_\beta(3\coth(\kappa) + \tanh(\kappa))}{36\kappa} + \frac{\alpha_\beta\big(108(\kappa-1) + \alpha_\beta\big(1-\alpha_\beta\big)\big(114 - 9\alpha_\beta - 15\alpha^2\big) - 8\kappa\alpha_\beta^4\big)}{36(\kappa-1)\kappa^2 f(\alpha_\beta)} \tag{151}$$

where we have adopted the notations

$$f(\alpha_\beta) = 36 - \alpha_\beta\big(38 - 3\big(1-\alpha_\beta\big)\alpha_\beta\big), \quad \kappa^2 = \frac{\alpha_\beta^2}{36}\xi \tag{152}$$

Appendix D. Lumped coefficients for periodic micro-structure

We define here the lumped mapping variable s^∞ by

$$s^\infty = \sum_{k=1}^{N_\mathcal{V}} s_k^\infty \tag{153}$$

Summing up the quasi-steady closure problems for s_k^∞, the closure problem for s^∞ reads

$$0 = \lambda_\beta \nabla^2 s^\infty - \alpha_\beta^{-1}\frac{A_p}{\mathcal{V}}\sum_{p=1}^{N_\mathcal{V}} h_p^\infty, \text{ in the } \beta\text{-phase} \tag{154}$$

$$s^\infty = 1, \text{ at } A_p \ 1 \le p \le N_\mathcal{V} \tag{155}$$

$$\text{Periodicity: } s^\infty(\mathbf{x} + \mathbf{r}) = s^\infty(\mathbf{x}) \tag{156}$$

$$\text{Average: } \langle s^\infty \rangle^\beta = 0 \tag{157}$$

where:

$$h_p^\infty = \sum_{k=1}^{N_\mathcal{V}} h_{pk}^\infty = -\frac{1}{A_p}\int_{A_p} \mathbf{n}\cdot\lambda_\beta \nabla s^\infty \, dS \tag{158}$$

Since the system illustrated in Fig. 1 is periodic in all directions, the value of h_p^∞ does not depend on the number of particles $N_\mathcal{V}$. As a result h_p^∞ can be calculated for a spatially periodic unit cell that contains solely one particle.

References

Anderson, T.B., Jackson, R., 1967. Fluid mechanical description of fluidized beds. Equations of motion. Ind. Eng. Chem. Fundam. 6 (4), 527–539.

Balachandar, S., Ha, M.Y., 2001. Unsteady heat transfer from a sphere in a uniform cross-flow. Phys. Fluids 13 (12), 3714–3728.

Boivin, M., Simonin, O., Squires, K.D., 1998. Direct numerical simulation of turbulence modulation by particles in isotropic turbulence. J. Fluid Mech. 375, 235–263.

Boivin, M., Simonin, O., Squires, K.D., 2000. On the prediction of gas–solid flows with two-way coupling using large eddy simulation. Phys. Fluids 12 (8), 2080–2090.

CALIF^{3}S: C++ Adaptive LIbrary For Fluid Flow Simulation, https://gforge.irsn.fr/gf/project/calif3s/.

Cannevière, K., 2003. Simulation Numérique Directe de la Combustion Turbulente Diphasique: Application à L'étude de la Propagation et de la Structure des Flammes. INSA de Rouen.

Capecelatro, J., Desjardins, O., 2013. An Euler–Lagrange strategy for simulating particle-laden flows. J. Comput. Phys. 238, 1–31.

Carbonell, R.G., Whitaker, S., 1984. Heat and mass transfer in porous media. In: Fundamentals of Transport Phenomena in Porous Media. Springer, Dordrecht, pp. 121–198.

Chang, H.C., 1983. Effective diffusion and conduction in two-phase media: a unified approach. AIChE J. 29 (5), 846–853.
Climent, E., Magnaudet, J., 2006. Dynamics of a two-dimensional upflowing mixing layer seeded with bubbles: bubble dispersion and effect of two-way coupling. Phys. Fluids 18 (10), 103304.
Cloney, C., Ripley, C., Pegg, M., Amyotte, P., 2018. Laminar burning velocity and structure of coal dust flames using a unity Lewis number CFD model. Combust. Flame 190, 87–102.
Crowe, C., Schwarzkopf, J., Sommerfeld, M., Tsuji, Y., 2011. Multiphase Flows with Droplets and Particles. CRC Press.
Cvetkovic, D., Cvetković, D.M., Rowlinson, P., Simic, S., 1997. Eigenspaces of Graphs, 66. Cambridge University Press.
D'Amico, M., Dufaud, O., Latché, J.C., Trélat, S., Perrin, L., 2016. Parametric study of the explosivity of graphite-metals mixtures. J. Loss Prev. Process Ind. 43, 714–720.
Davit, Y., Bell, C., Byrne, H., Chapman, L., Kimpton, L., Lang, G., Leonard, K., Oliver, J., Pearson, N., Shipley, R., Waters, S., Whiteley, J., Wood, B., Quintard, M., 2013. Homogenization via formal multiscale asymptotics and volume averaging: how do the two techniques compare? Adv. Water Resour. 62, 178–206.
Davit, Y., Quintard, M., 2012. Comment on frequency-dependent dispersion in porous media. Phys. Rev. E 86 (1), 013201.
Davit, Y., Quintard, M., 2015. Handbook of Porous Media. Taylor & Francis.
Denkevits, A., Dorofeev, S., 2005. Dust explosion hazard in ITER: explosion indices of fine graphite and tungsten dusts and their mixtures. Fusion Eng. Des. 75–79, 1135–1139.
Feng, Z.G., Michaelides, E.E., 1996. Unsteady heat transfer from a sphere at small Peclet numbers. J. Fluids Eng. 118 (1), 96–102.
Gray, W.G., 1975. A derivation of the equations for multi-phase transport. Chem. Eng. Sci. 30 (2), 229–233.
Gunn, D.J., 1978. Transfer of heat or mass to particles in fixed and fluidised beds. Int. J. Heat Mass Transf. 21 (4), 467–476.
Horn, R.A., Johnson, C.R., 1990. Matrix Analysis. Cambridge University Press.
Janeschitz, G., 2001. Plasma-wall interaction issues in ITER. J. Nucl. Mater. 290–293, 1–11.
Kriebitzsch, S.H.L., Van der Hoef, M.A., Kuipers, J.A.M., 2013. Drag force in discrete particle models – continuum scale or single particle scale? AIChE J. 59 (1), 316–324.
Ling, Y., Balachandar, S., Parmar, M., 2016. Inter-phase heat transfer and energy coupling in turbulent dispersed multiphase flows. Phys. Fluids 28 (3), 1–26.
Magnus, W., 1954. On the exponential solution of differential equations for a linear operator. Commun. Pure Appl. Math. 7 (4), 649–673.
Michaelides, E.E., Feng, Z., 1994. Heat transfer from a rigid sphere in a nonuniform flow and temperature field. Int. J. Heat Mass Transf. 37 (14), 2069–2076.
Moyne, C., 1997. Two-equation model for a diffusive process in porous media using the volume averaging method with an unsteady-state closure. Adv. Water Resour. 20 (2–3), 63–76.
Neophytou, A., Mastorakos, E., 2009. Simulations of laminar flame propagation in droplet mists. Combust. Flame 156, 1627–1640.
Park, H.Y., Park, Y.H., 2016. Laminar burning velocities of atmospheric coal air mixtures. J. Electr. Power Energy 2 (1), 89–96.
Piar, L., Babik, F., Herbin, R., Latché, J.-C., 2013. A formally second-order cell centred scheme for convection–diffusion equations on general grids. Int. J. Numer. Methods Fluids 71 (7), 873–890.
Proust, C., 2017. Turbulent flame propagation in large dust clouds. J. Loss Prev. Process Ind. 49, 859–869.
Quintard, M., Kaviany, M., Whitaker, S., 1997. Two-medium treatment of heat transfer in porous media: numerical results for effective properties. Adv. Water Resour. 20 (2–3), 77–94.
Quintard, M., Whitaker, S., 1993a. One-and two-equation models for transient diffusion processes in two-phase systems. In: Advances in Heat Transfer, 23. Elsevier, pp. 369–464.
Quintard, M., Whitaker, S., 1993b. Transport in ordered and disordered porous media: volume-averaged equations, closure problems, and comparison with experiment. Chem. Eng. Sci. 48 (14), 2537–2564.
Quintard, M., Whitaker, S., 1994a. Transport in ordered and disordered porous media I: the cellular average and the use of weighting functions. Transp. Porous Med. 14 (2), 163–177.
Quintard, M., Whitaker, S., 1994b. Transport in ordered and disordered porous media III: closure and comparison between theory and experiment. Transp. Porous Med. 15 (1), 31–49.
Quintard, M., Whitaker, S., 1995. Local thermal equilibrium for transient heat conduction: theory and comparison with numerical experiments. Int. J. Heat Mass Transf. 38 (15), 2779–2796.
Quintard, M., Whitaker, S., 2000. Theoretical Analysis of Transport in Porous Media. Marcel Dekker Inc., New York.
Ranz, W.E., Marshall, W.R., 1952. Evaporation from drops. Chem. Eng. Progr. 48 (3), 141–146.
Silvestrini, M., Genova, B., Trujillo, F.J.L., 2008. Correlations for flame speed and explosion overpressure of dust clouds inside industrial enclosures. J. Loss Prev. Process Ind. 21, 374–392.
Simonin, O., 1996. Continuum modelling of dispersed two-phase flows. In: Combustion and Turbulence in Two-Phase Flows. In: Lecture Series – von Karman Institute for Fluid Dynamics. Rhode Saint Genèse (Belgium), pp. K1–K47.
Simonin, O., Deutsch, E., Minier, J.P., 1993. Eulerian prediction of the fluid/particle correlated motion in turbulent two-phase flows. Appl. Sci. Res. 51 (1–2), 275–283.
Sun, B., Tenneti, S., Subramaniam, S., 2015. Modeling average gas–solid heat transfer using particle-resolved direct numerical simulation. Int. J. Heat Mass Transf. 86, 898–913.
Thiam, E.I., Masi, E., Climent, E., Simonin, O., Vincent, S., 2019. Particle-resolved numerical simulations of the gas–solid heat transfer in arrays of random motionless particles. Acta Mech. 230 (2), 541–567.
Whitaker, S., 1972. Forced convection heat transfer correlations for flow in pipes, past flat plates, single cylinders, single spheres, and for flow in packed beds and tube bundles. AIChE J. 18 (2), 361–371.
Whitaker, S., 1985. A simple geometrical derivation of the spatial averaging theorem. Chem. Eng. Educ. 19 (1), 18–21, 50–52.
Whitaker, S., 1998. Coupled transport in multiphase systems: a theory of drying. Adv. Heat Transf. 31, 1–104.
Zanotti, F., Carbonell, R.G., 1984. Development of transport equations for multiphase system-I: general development for two phase system. Chem. Eng. Sci. 39 (2), 263–278.
Zhang, D.Z., Prosperetti, A., 1997. Momentum and energy equations for disperse two-phase flows and their closure for dilute suspensions. Int. J. Multiph. Flow 23 (3), 425–453.
Zhang, H.Y., Huang, X.Y., 2001. A two-equation analysis of convection heat transfer in porous media. Transp. Porous Med. 44 (2), 305–324.